

Validation of the coupled Eta/SSiB model over South America

Sin Chan Chou

Centro de Previsão de Tempo e Estudos Climáticos (CPTEC), Instituto Nacional de Pesquisas Espaciais (INPE), Cachoeira Paulista, São Paulo, Brazil

Clemente A. S. Tanajura

Laboratório Nacional de Computação Científica (LNCC), Petrópolis, Rio de Janeiro, Brazil

Yongkang Xue

Department of Geography, University of California at Los Angeles (UCLA), Los Angeles, California, USA

Carlos A. Nobre

Centro de Previsão de Tempo e Estudos Climáticos (CPTEC), Instituto Nacional de Pesquisas Espaciais (INPE), Cachoeira Paulista, São Paulo, Brazil

Received 18 December 2000; revised 25 June 2001; accepted 3 August 2001; published 25 October 2002.

[1] Two 1-month integrations were performed with the regional Eta model coupled with the Simplified Simple Biosphere model (SSiB) over South America. The goal of the present work is to validate the model and to investigate its biases and skill on the simulations of South American climate. This is an initial step on the use of this model for climate research. The Eta model was set up with 80-km horizontal resolution and 38 vertical layers over the South American continent and part of the adjacent oceans. Analyses from the National Centers for Environmental Prediction (NCEP) were used as initial and lateral boundary conditions. The selected months were August and November 1997, which are in opposite phases of the precipitation annual cycle observed in the central part of South America. The model was integrated continuously for each 1-month period. Monthly means and daily variations of simulated precipitation and surface temperature compare well with observations. The patterns of simulated outgoing longwave radiation are also similar to the observed ones. However, a positive bias is verified in the simulations. The model shows a positive bias in latent and sensible heat surface fluxes due to an excessive shortwave incoming radiation at the surface. Comparisons with a version of the Eta model coupled with the bucket model shows that the Eta/SSiB version improves the surface temperature and increases precipitation in the interior of the continent during wet months. *INDEX TERMS:* 3322 Meteorology and Atmospheric Dynamics: Land/atmosphere interactions; 3337 Meteorology and Atmospheric Dynamics: Numerical modeling and data assimilation; 3354 Meteorology and Atmospheric Dynamics: Precipitation (1854)

Citation: Chou, S. C., C. A. S. Tanajura, Y. Xue, and C. A. Nobre, Validation of the coupled Eta/SSiB model over South America, *J. Geophys. Res.*, 107(D20), 8088, doi:10.1029/2000JD000270, 2002.

1. Introduction

[2] During austral summer, the precipitation maximum over South America is located in the southern part of the Amazon river basin. During winter, the dry season is evident in the central region of tropical South America, and the precipitation maximum in the sector is located in Central America. These are opposite phases of the strong annual cycle of precipitation in the region. The transition from one phase to the other occurs generally within less than a month period [Horel *et al.*, 1989].

[3] Other features also characterize South American climate [Satyamurty *et al.*, 1998]. During the summer, in

general, the South Atlantic Convergence Zone (SACZ) is formed and is responsible for the precipitation maximum in the central and southeastern parts of the continent. The SACZ is associated with the Bolivian High and the convective activity over the Amazon [Figueroa *et al.*, 1995; Liebmann *et al.*, 1999]. During the winter, high surface pressures prevail over the central part of the continent. This influences the trajectories of the frontal systems and causes the precipitation maximum over southern Brazil.

[4] Despite the remarkable precipitation signature, the correct precipitation distribution over South America is hardly obtained by spectral general circulation models (GCMs) which are commonly used for weather and climate predictions. This occurs mostly because of their relatively low resolution. To improve the GCMs precipitation and circulation representations over specific areas, higher reso-

lution regional models nested in GCMs and/or analyses can be used. High-resolution regional models may better represent mesoscale processes, topography, coastal geometry, and land surface characteristics than GCMs. This may provide a more realistic model simulation and improve predictability.

[5] *Dickinson et al.* [1989], *Giorgi and Bates* [1989], and *Giorgi* [1990] were the first to use regional models for climate studies. They took the Pennsylvania State University/National Center for Atmospheric Research Mesoscale Model MM4 to detail the simulations from the Climate Community Model over the western United States. This region was selected mostly because of the complex terrain. Their goal was to study weather and winter climate with integrations ranging from 3–5 days to 1 month. They discussed the need of realistic large-scale GCM solutions for a good regional model performance. They also discussed the usefulness of the regional models as tool to improve climate predictability.

[6] *Fennessy and Shukla* [2000] could simulate North American summer and winter precipitation distribution and its interannual variability with the regional Eta model. *Ji and Vernekar* [1997] also found improvements on the Eta model representation of the Indian Monsoon System and its variability due to ENSO with respect to the GCM simulation. The regional model domain in these studies was large. *Seth and Giorgi* [1998], *Fennessy and Shukla* [2000], and others observed that the regional model solution depends on the domain size.

[7] The capacity of regional models to improve GCM climate simulations is not easy to assess due to various aspects of regional climate modeling such as resolution, lateral boundary conditions, initialization, spin-up time and model variability [*Giorgi and Mearns*, 1999; *Weisse et al.*, 2000]. The Project to Intercompare Regional Climate Simulations (PIRCS) [*Takle et al.*, 1999] evaluated various regional models and focused on the 1988 drought period over the central United States. The results showed that all models could capture large-scale patterns, but diverged during periods strongly affected by shortwave lows. The models exhibited substantial differences in the simulated surface fluxes among themselves and with respect to observations, in such a way that all models showed weaknesses and strengths.

[8] *Pan et al.* [1999] discussed the regional model sensitivity to reinitializations during 1-month integrations over North America. Since the regional models have different resolution and often different physics from the GCMs, which they are nested in, there is a spin-up period required by the regional model to adjust to the initial condition. This was also observed by *Tanajura* [1996] and *Tanajura and Shukla* [2000]. They carried out 3-month simulations with the regional Eta model reinitialized every 48 hours to investigate South American summer climate and the influence of the Andes in this climate. The SACZ, the Bolivian High, and the contrasting high and low rainfall rates between the Amazon region and northeast Brazil were simulated. The absence of the Andes reduced the surface sensible heat fluxes over the Bolivian Plateau.

[9] *Chou et al.* [2000] also used the Eta model over South America to detail the CPTEC/COLA (Centro de Previsão de Tempo e Estudos Climáticos/Center for Ocean-Land-Atmosphere Studies) GCM [*Bonatti*, 1996] forecasts during

opposite phases of the precipitation annual cycle. The Eta model was integrated without reinitialization for the months of August and November 1997, and used CPTEC/COLA GCM forecasts as lateral boundary conditions. It was shown that the regional model provided higher equitable threat scores and smaller precipitation biases than the GCM.

[10] These previous works have shown that the Eta model is a valuable tool to investigate South American climate. However, the model version used in some of the papers mentioned above had a relatively simple land hydrology scheme, the so-called bucket model [*Manabe*, 1969]. This model may not be appropriate for studies over South America where one third of the continent is covered by rain forest. This indicates that land surface processes are important forcings to the South America weather and climate.

[11] Here, the Eta model is coupled with a simplified version of *Sellers et al.* [1986] Simplified Simple Biosphere model (SSiB) [*Xue et al.*, 1991]. This model is here referred to as the Eta/SSiB model. SSiB explicitly takes into account vegetation and soil heterogeneities. When the model was coupled with the COLA GCM, it produced a more realistic partition of energy at the land surface in comparison to the bucket hydrology [*Sato et al.*, 1989; *Xue et al.*, 1996].

[12] In this study, the Eta/SSiB model is validated over South America by performing 1-month integrations. The selected months were August and November 1997, the same months used by *Chou et al.* [2000]. The results are verified with observations, reanalyses, and compared with the Eta model using the bucket hydrology and the CPTEC/COLA GCM simulations.

[13] The present work is part of the hydrometeorological component of the Large-Scale Biosphere-Atmosphere Experiment in Amazonia (LBA). The Eta/SSiB model is being prepared for studies of the seasonal-to-interannual variability of the Amazon hydrological cycle. The LBA aims at improving the understanding of the climatological, hydrological, and biogeophysical systems of the Amazon, the impact of land-cover change, and the interactions between the Amazon and the Earth system. Future works using Eta/SSiB model will focus on the impact of land surface processes on the South American annual water cycle and deforestation effects.

[14] The models and the integration procedures used in this paper are described in section 2. Model output is validated in section 3, and comparison with other model results are done in section 4. Sensitivity to different boundary conditions in long-term integrations are assessed in section 5. Discussions and conclusions are in section 6.

2. Methodology

2.1. The Eta Model

[15] The NCEP Eta model is an operational short-range forecasting model used over the North and South American regions [*Mesinger et al.*, 1988; *Janjić*, 1994; *Black*, 1994].

[16] Finite difference schemes are applied to the model system of equations in space and time. The discretization of the domain is done with the semistaggered Arakawa E-grid in the horizontal and the Lorenz grid in the vertical. The following numerical methods are used in the model: (1) a horizontal advection scheme developed by *Janjić* [1984] that conserves momentum and energy, and restricts the

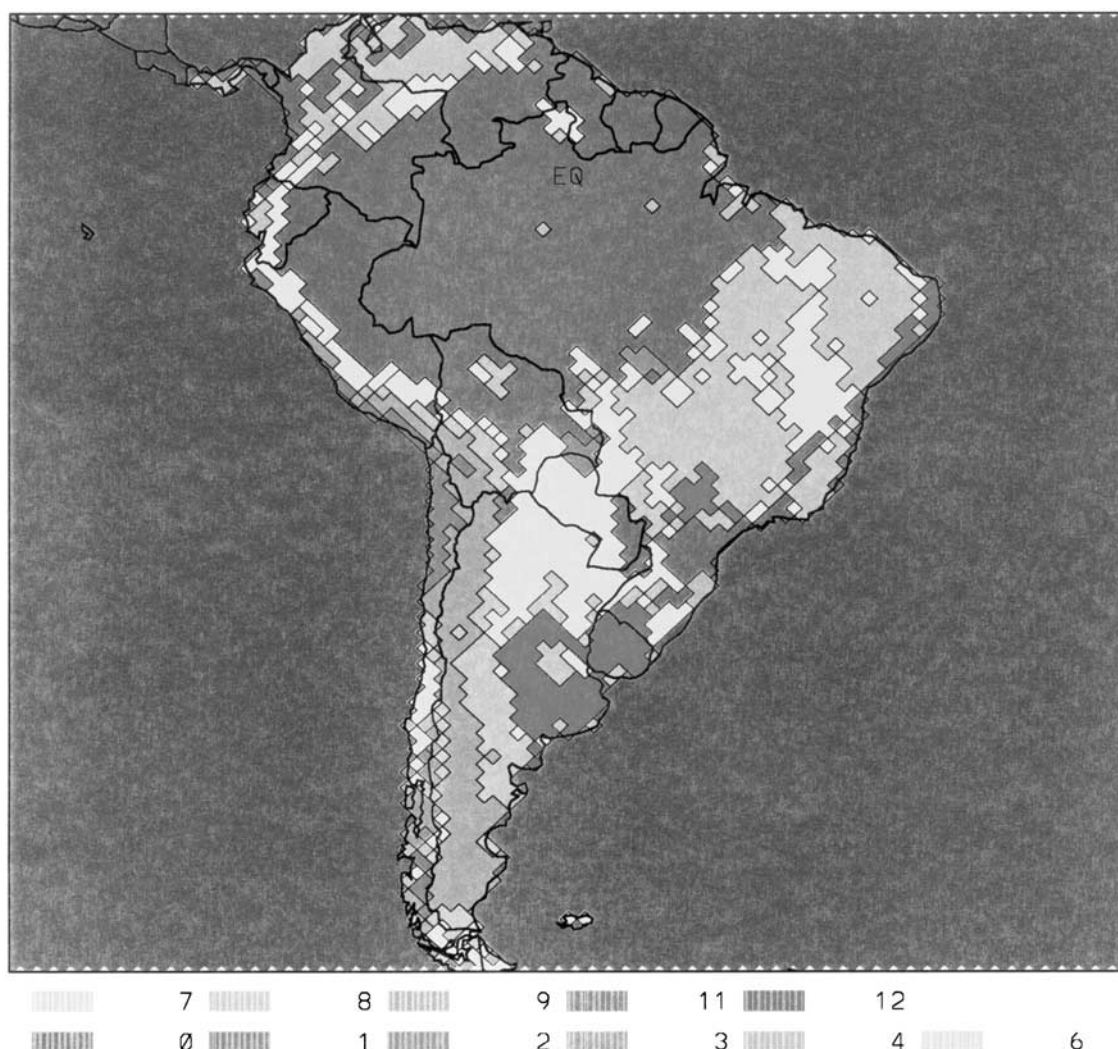


Figure 1. 80-km vegetation map derived from an original 1-km University of Maryland data set. See color version of this figure at back of this issue.

cascade of energy toward the smaller scales; (2) second order nonlinear lateral diffusion depending on the turbulent kinetic energy; (3) a forward-backward scheme for the inertia-gravity wave modified to [Mesinger, 1977; Janjić, 1979] to prevent the gravity wave separation; and (4) a split-explicit time differencing with time step of the advection terms twice of the inertia-gravity wave terms.

[17] The resolution used in the Eta model was 80 km in the horizontal and 38 layers in the vertical, with higher resolution in the boundary layer and in the upper troposphere/lower stratosphere. The Eta model domain is positioned approximately within about 57°S to 13°N and about 100°W to 20°W, centered at 22°S, 60°W.

[18] One of the features of this model is the vertical coordinate, η [Mesinger, 1984], defined as

$$\eta = \frac{p - p_t}{p_s - p_t} \frac{p_r(z) - p_t}{p_r(0) - p_t}, \quad (1)$$

where p is the pressure, subscripts s , t , and r , refer to the surface, the top of the atmosphere, and a reference state,

respectively, and z is the height. This coordinate has relatively horizontal surfaces at all times and orography is represented by step-like functions. With this system, errors associated with the determination of the pressure gradient force along a steeply sloped coordinate surface are minimized. The η coordinate becomes appropriate for simulation over South America because the Andes Cordillera has very steep slopes along most of its longitudinal extension.

[19] The physics of the model contains: (1) the Betts–Miller cumulus parameterization modified to include precipitation efficiency [Betts and Miller, 1986; Janjić, 1994]; (2) a Mellor–Yamada level 2.5 to account for turbulence between the model layers inside the boundary layer and in the free atmosphere; and (3) a Mellor–Yamada level 2.0 to account for turbulence in the lowest model layer. Turbulent kinetic energy is calculated at model layer interfaces and is used to compute the exchange coefficients for the transfer of heat, moisture and momentum.

[20] The radiation package uses the schemes of *Lacis and Hansen* [1974] and *Fels and Schwarzkopf* [1975] for the shortwave and the longwave radiation, respectively. Both

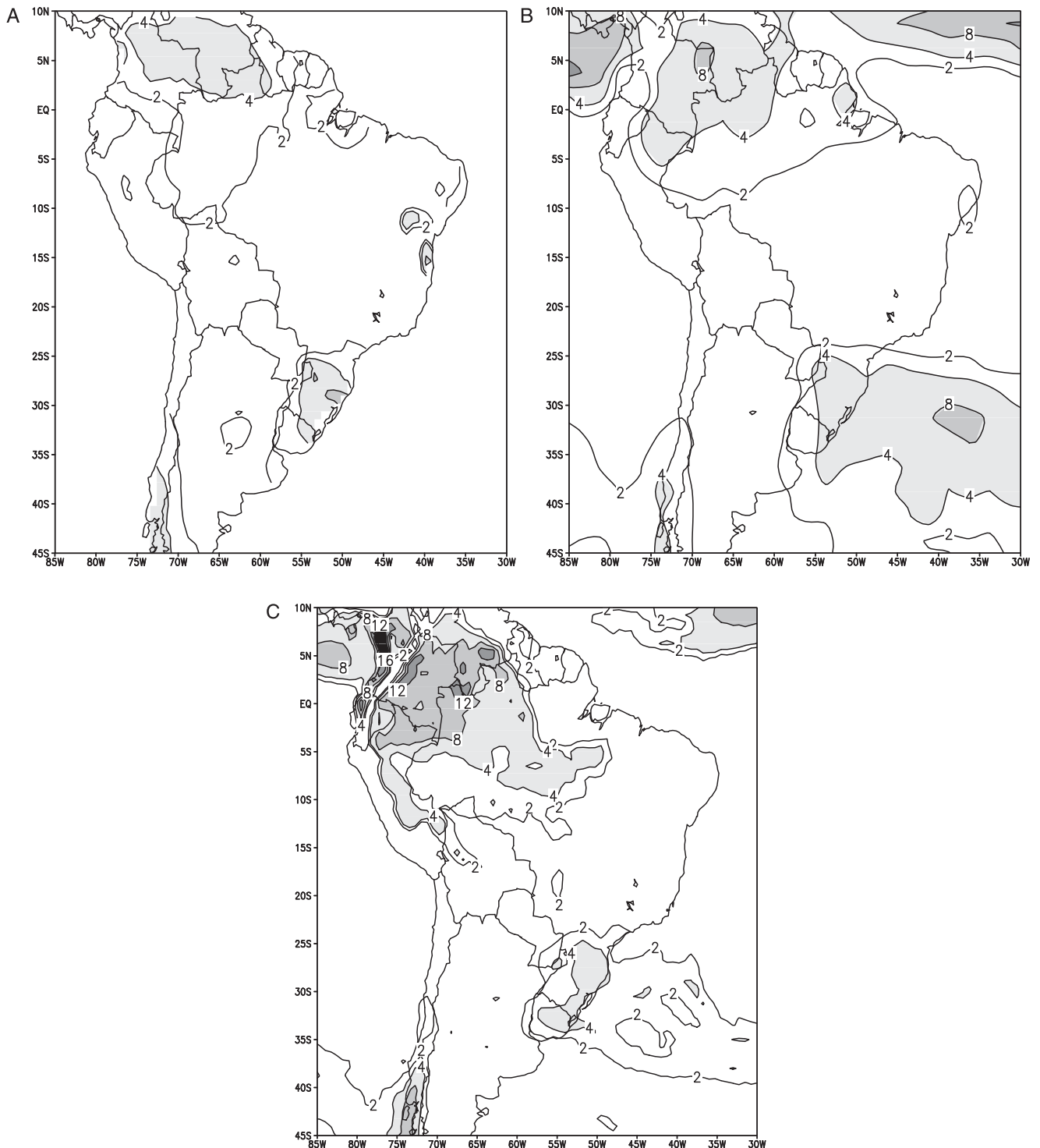


Figure 2. August 1997 mean precipitation (mm d^{-1}) from (a) Xie and Arkin data set, (b) surface observations, and (c) Eta/SSiB simulation.

stratiform and cumuliform interactive clouds are diagnosed [Slingo, 1987] based upon the model relative humidity and convective rainfall rate.

[21] Surface fluxes of momentum, sensible heat, latent heat, and radiation over land are nonlinearly determined by the interaction between the lowest model layer with the SSiB, which is summarized below. Over ocean areas, the surface fluxes are determined using Monin–Obukhov

theory according to *Lobocki* [1993]. Boundary conditions for the Eta model include sea surface temperature and orography.

2.2. The Simplified Simple Biosphere Model

[22] SSiB model is a simplified version of the model developed by *Sellers et al.* [1986]. It recognizes 12 different vegetation types according to *Dorman and Sellers* [1989],

and it is set up with 3 soil layers and 1 canopy layer. A 1-km resolution vegetation mask produced by the department of geography at the University of Maryland, College Park, USA [Hansen *et al.*, 2000], was used to create the vegetation distribution in the Eta model domain. The vegetation mask is shown in Figure 1, and was obtained under the criteria of the predominant vegetation type within a predominant land-cover group in each grid-box. The land-cover groups are trees, shrubs, grass and bare soil. In this mask, the rain forest vegetation type covers about a third of the continent, the second most frequent type is the type 8, the broadleaf shrubs with groundcover.

[23] SSiB model has 8 prognostic variables: soil wetness for 3 layers; temperatures at the canopy, ground surface and deep soil layers; snow depth at the ground; and intercepted water by the canopy. Implicit backward scheme is used to calculate the temperature tendency in the coupling of the lowest atmospheric model layer with SSiB model, such that energy conservation between the land surface and the atmosphere is satisfied. Soil temperature is calculated by the force-restore method and water movement in the soil is described by diffusion equation. Each vegetation type has a set of parameters to describe the plant physiology. Many parameters have been calibrated using measurements taken in the Amazon region [Xue *et al.*, 1996].

2.3. The Integrations

[24] The model was integrated continuously for the months of August and November 1997. The National Centers for Environmental Prediction (NCEP) T062L28 analyses were used for initial and lateral boundary conditions. The latter were updated every 6 hours. Observed sea surface temperatures were taken on 1 August 1997, and on 1 November 1997, and kept constant during the integrations. The actual initial conditions started on 0000 UTC 29 July 1997 and 0000 UTC 28 October 1997, and three days of model spin-up time were excluded from results. The available data for the soil moisture initial condition was the annual climatology. Seth and Giorgi [1998] have done experiments on the sensitivity of initial soil moisture and two domain sizes in limited area models. They showed that in the largest domain, the simulations are more sensitive to soil moisture. This is because the control exerted by the lateral boundary conditions had been moved away from the region of interest. In the current simulations it is expected that the soil moisture plays its importance as most of the lateral boundaries are relatively far from the continent.

3. Model Validation

3.1. Precipitation

[25] During the dry month, August 1997, mean precipitation over land was observed mainly over three regions: the northernmost part of South America, the southern Brazilian regions, and Chile, south of 35°S. Different weather regimes are responsible for this precipitation pattern. In the northern part, rainfall is produced by tropical convection, and interactions between surface heating and large-scale convergence. In the southern part, rainfall is produced by frontal passages and mountain blocking effects. Figures 2a and 2b show the mean observed precipitation from two different sources. The former is from

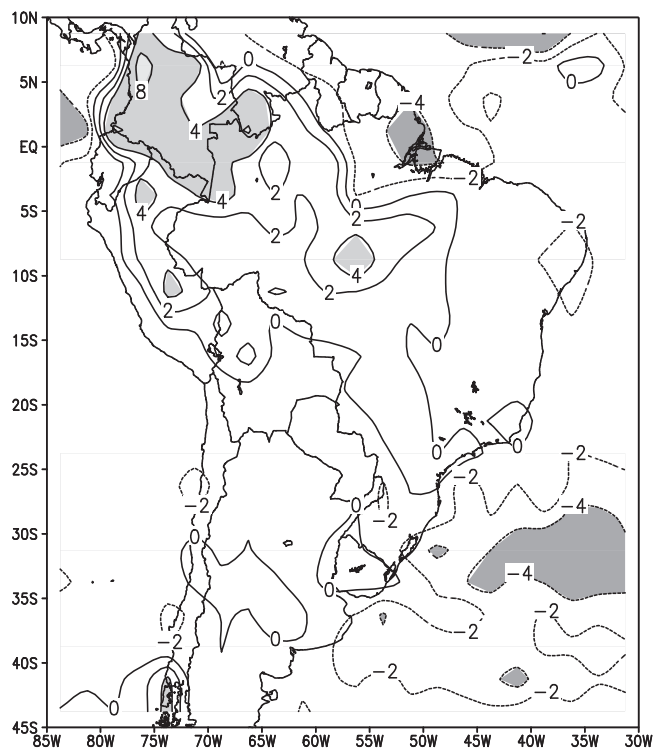


Figure 3. Difference between model and Xie and Arkin mean precipitation (mm d^{-1}) for August 1997.

blended in situ and remote sensed data as described by Xie and Arkin [1996], and the latter is from surface ground-based station data. The overall pattern and magnitude of these precipitation data are similar, however, some differences can be noticed. In Figure 2a, there is a local maximum over the eastern coast between 10°S and 15°S, which is absent in Figure 2b. Also, in the equatorial region, rainfall is smaller in the station data than in the Xie and Arkin data. The latter has low resolution, $2.5^\circ \times 2.5^\circ$, but covers ocean areas. The ground-based station data are restricted to Brazil, contain monthly totals, and are quality controlled by the Brazilian National Meteorological Service. However, they are unevenly distributed, since there are few stations in the Amazon and central Brazil.

[26] The Eta/SSiB model simulation for August 1997 (Figure 2c) captured closely the observed pattern with higher spatial variability. In the northern part near the Colombian Andes, the amounts were slightly overestimated. However, climatology shows that heavy rainfall is commonly found in those regions [Figueroa and Nobre, 1990]. The low resolution of the observational data may have missed the highest values. The Intertropical Convergence Zone (ITCZ) over the Pacific and Atlantic Oceans were correctly positioned by the model. The precipitation band over the Atlantic Ocean, between 25°S and 40°S, was also positioned correctly but underestimated by up to 6 mm d^{-1} . The differences between model and Xie and Arkin precipitation are shown in Figure 3. To take the difference, model data were interpolated to the Xie and Arkin data resolution, which is 2.5° in longitude and latitude.

[27] During the wet month, November 1997, precipitation was observed mostly over the central part of the

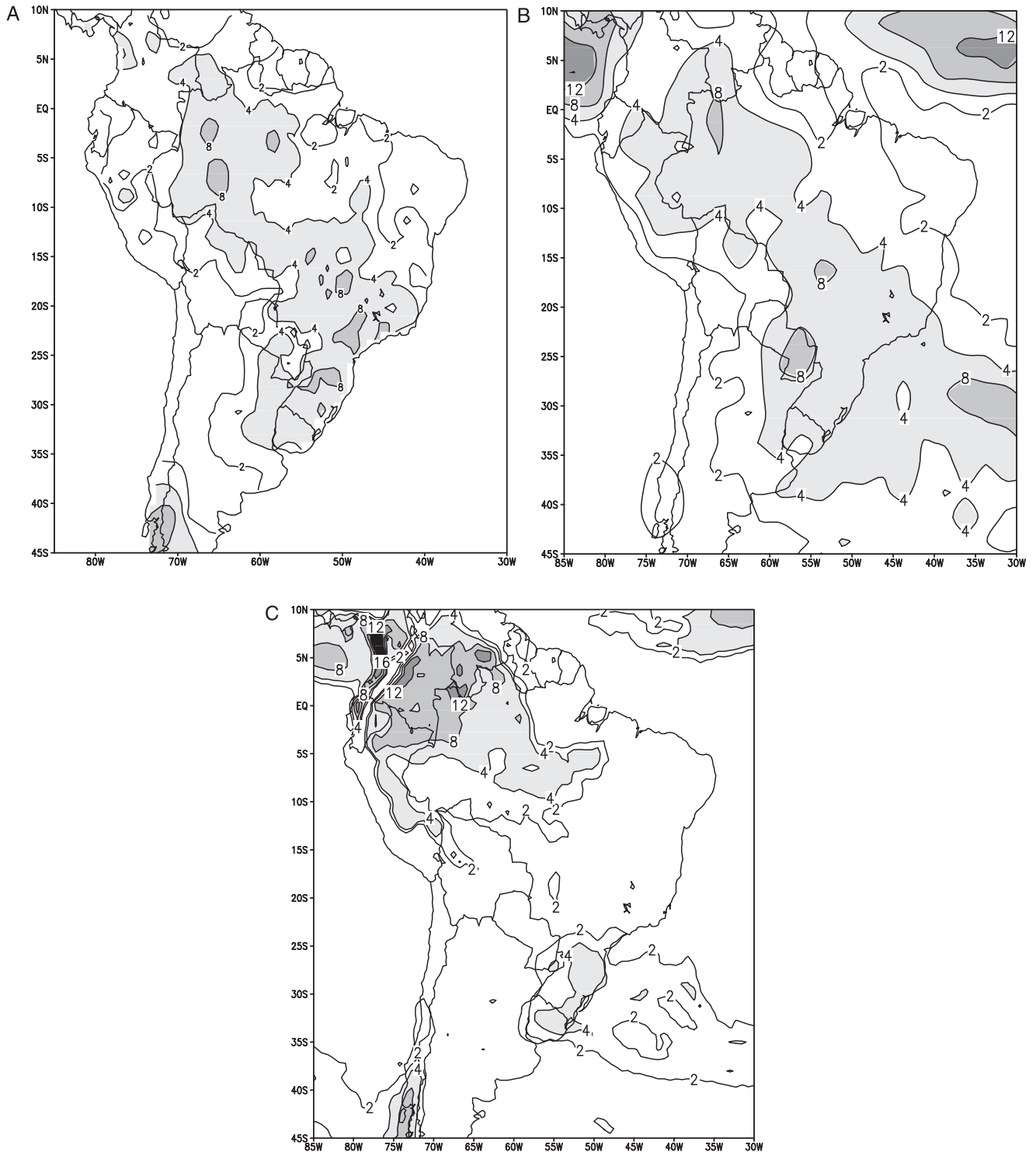


Figure 4. Same as Figure 2, except for November 1997.

continent forming a continuous northwest-southeast oriented band with various local maxima (Figures 4a and 4b). Convection in the ITCZ is more active relatively to August. Comparing the two observational data sets, precipitation over southern Chile from the station data is larger than estimated from the Xie and Arkin data.

[28] Similarly to August 1997, the model simulation (Figure 4c) captured the major features of the observed

precipitation pattern. The model produced relatively intense precipitation over southeastern Brazil, which was also found in the ground station data. A maximum over Paraguay, around 57°W and 25°S, observed only in the Xie and Arkin data, was well simulated by the model. The tropical weather regime over northeast Brazil is distinct from the one over the tropical Amazon region. The precipitation borderline between these two regimes, which can be characterized by

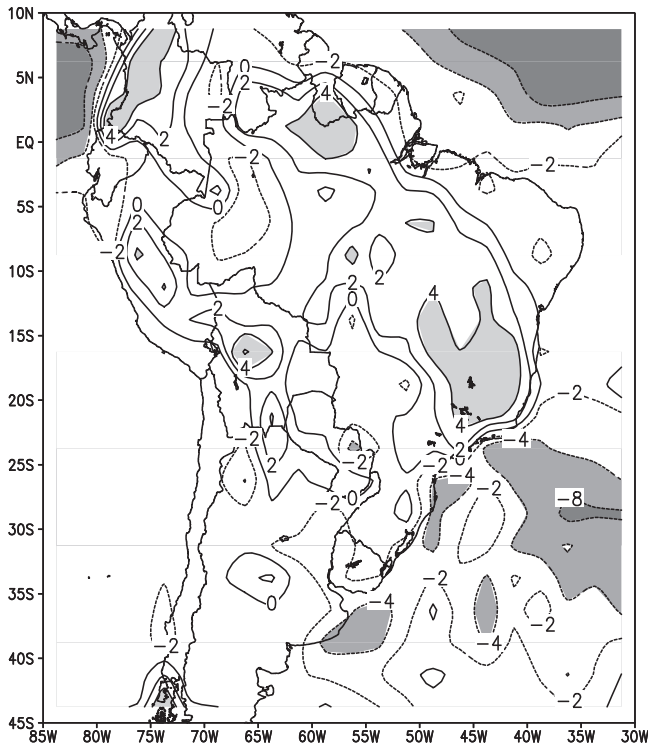


Figure 5. Difference between model and Xie and Arkin mean precipitation (mm d^{-1}) for November 1997.

the 2 mm d^{-1} contour line, is correctly simulated. However, the area in which precipitation is larger than 4 mm d^{-1} is broader in the simulation. The model underestimated the precipitation amounts over the ocean, as in August. The absence of model precipitation over the Atlantic ITCZ was partially caused by subsidence induced from the enhanced convection generated by the model over the continent. The differences between model and Xie and Arkin precipitation are shown in Figure 5.

[29] The daily variability of the model precipitation was also assessed. Two areas with distinct vegetation covers and

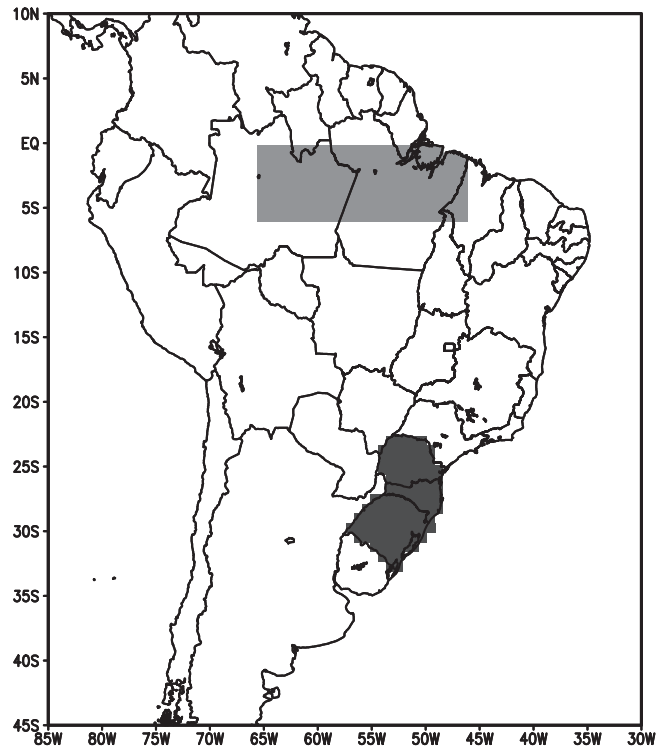


Figure 6. Validation regions. The light gray area covers part of the Amazon River basin and represents tropical area of broadleaf evergreen forest, and the dark gray area encompasses the Brazilian South region and represents a subtropical area with cultivation.

weather regimes were chosen. These areas are displayed in Figure 6. The northern area is covered by tropical rain forest and contains part of the Amazon river basin. The other area is covered by shrubs and cultivation and it is located over southern Brazil.

[30] Area average of daily accumulated precipitation from model and station data is shown for these two regions (Figure 7). Although the model produces reasonable

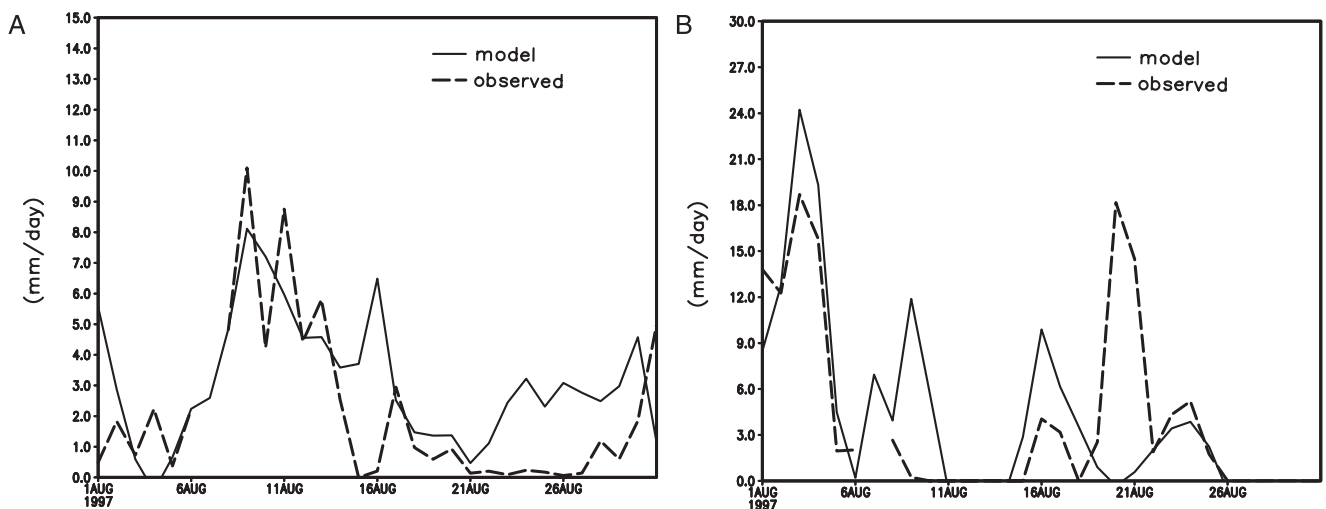


Figure 7. Daily series of August 1997 precipitation averaged over (a) the light gray area in Figure 6 and (b) the dark gray area. Units: mm d^{-1} .

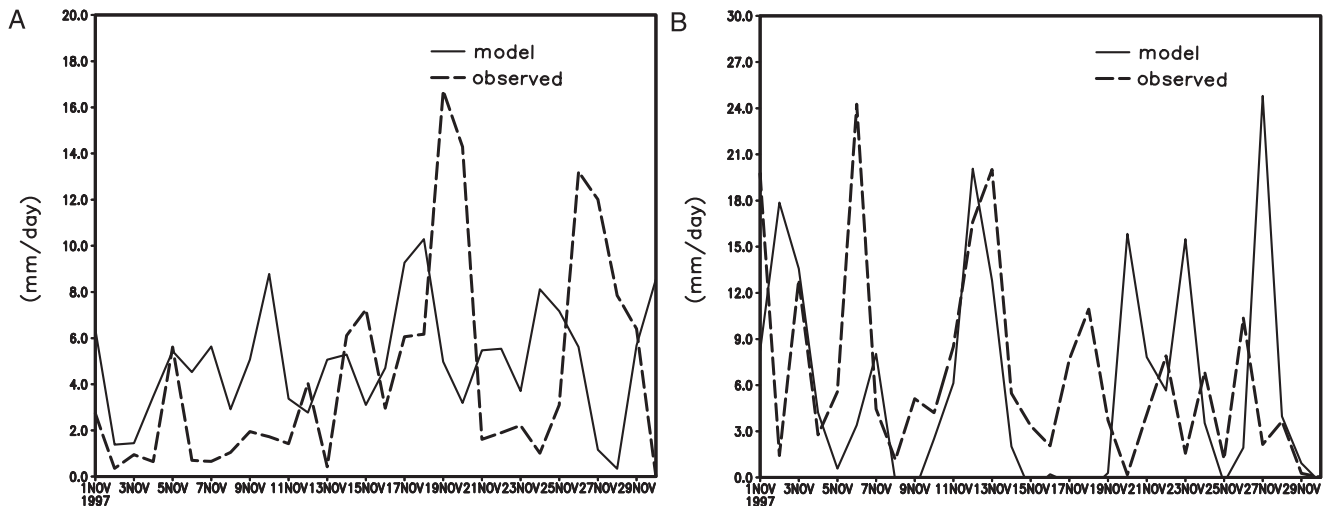


Figure 8. Same as Figure 7, except for November 1997.

monthly means, the simulations of daily variability in precipitation need to be further improved for August 1997. In the tropical region, the model performed well in the first 14 days of integration. In the subtropical region, the passage of two frontal systems produced heavy precipitation, one in the beginning of the month, which was well simulated by the model, and the other around 20 August, which was also simulated but positioned behind the observed frontal system by about 2 latitudinal degrees, remaining out of the selected subtropical region. The choice of the evaluation areas is not straightforward. A larger area in the latter case would have improved the results, however, it could also have smoothed them out.

[31] During November 1997, the total amount of precipitation increased in both tropical and subtropical regions (Figures 8a and 8b). The model daily variability was not captured as closely as in August 1997. In the tropics, the model seems to be leading observations, whereas in the subtropics this behavior is not clear. Most of rain during this wet month is produced from deep convection, in both tropical and subtropical regions. The reduced predictability may be due to model parameterization limitations in correctly simulating the thermodynamic structure of the atmosphere during those predominantly deep convective events.

3.2. Precipitation Score

[32] Precipitation is quantitatively assessed through the equitable threat score (ETS) and the bias score (BIAS). The ETS is given by [e.g., Mesinger and Black, 1992]:

$$ETS = \frac{H - CH}{S + O - H - CH} \quad (2)$$

where S is the number of simulated precipitation events above a certain threshold, O is the number of observed events above the threshold, H is the number of hits, N is the number of grid points in the validation, and $CH = (S \times O) / N$. The bias score is defined as: $BIAS = S/O$. ETS varies from 0 to 1, with higher values indicating better simulations. ETS and BIAS are used in combination. A perfect simulation would be equivalent to $ETS = 1$ and $BIAS = 1$.

[33] The monthly total precipitation was divided into 8 thresholds: 9, 30, 50, 100, 200, 300, 400, and 600 mm. The observed and the regional model monthly total precipitation fields were interpolated, by the kriging and linear methods,

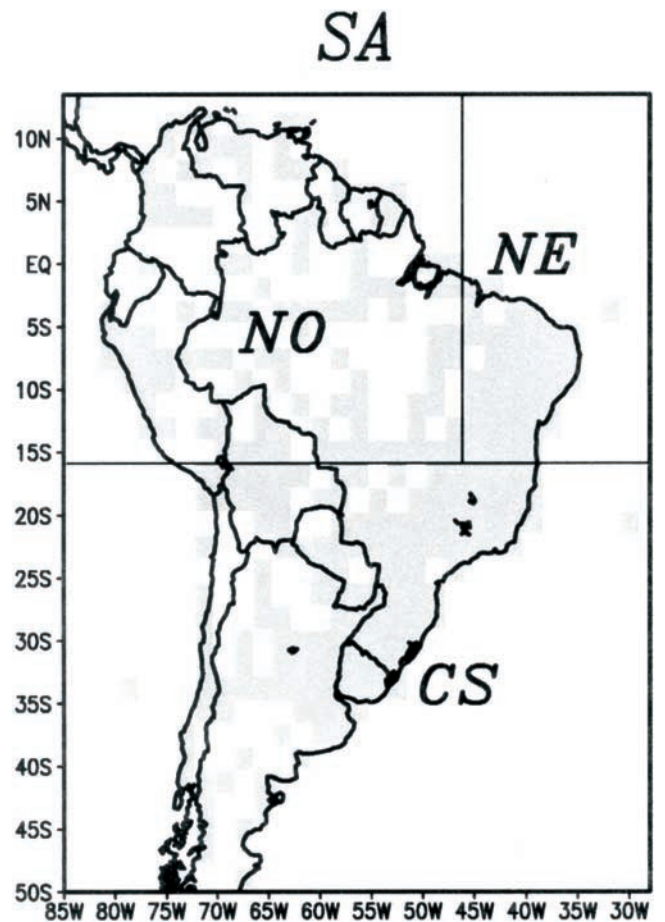


Figure 9. Regions where equitable threat scores are calculated. SA refers to the whole South America domain, NO to North, NE to Northeast, and CS to Center-South regions, as defined in the text.

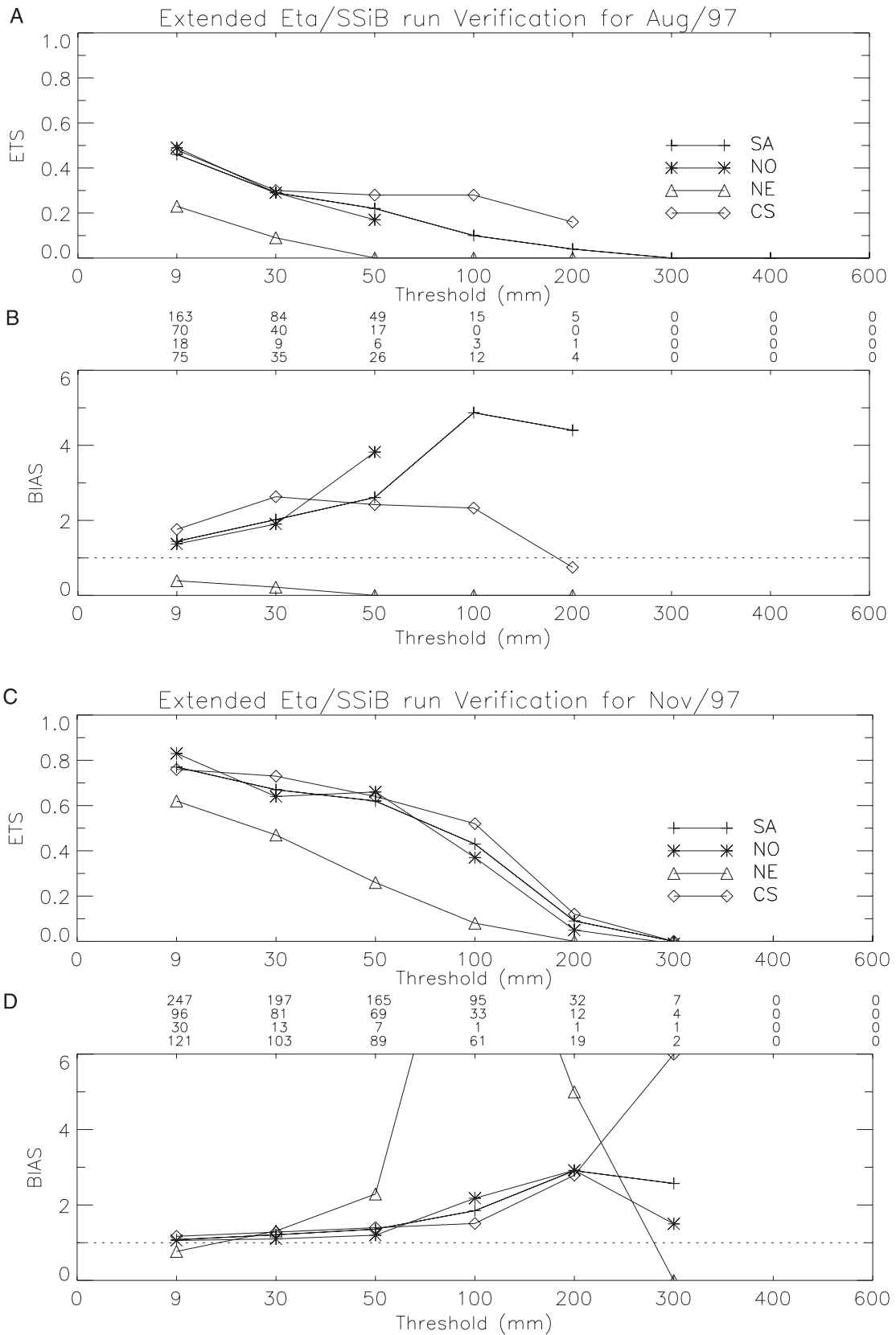


Figure 10. Equitable threat score and bias score for monthly total simulated precipitation for August 19, 97 in (a) and (b), respectively, and for November 1997 in (c) and (d), respectively. Regions are defined in the text and in Figure 9. The numbers in the first line below the x axis refer to the precipitation thresholds. The numbers in the lines immediately below refer to the number of observations found in each precipitation found in each precipitation threshold.

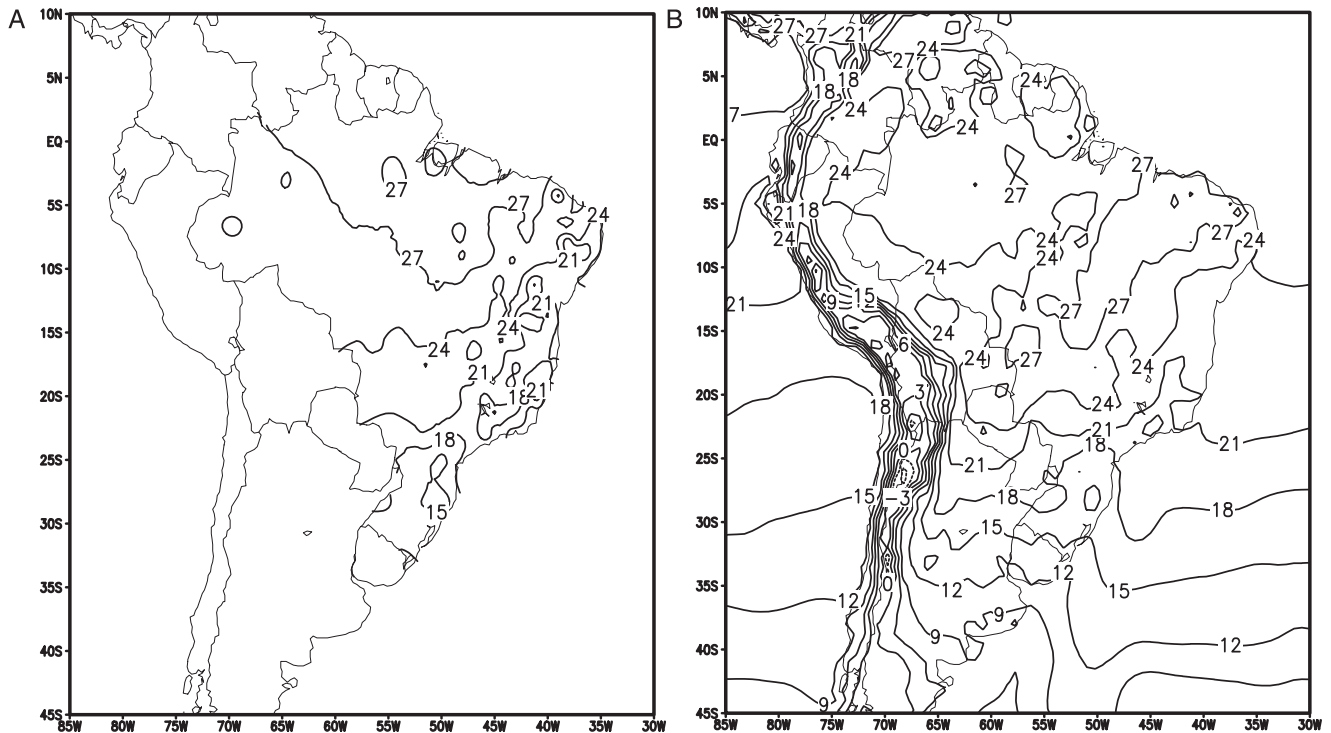


Figure 11. August 1997 mean surface temperature ($^{\circ}\text{C}$): (a) observed and (b) simulated.

respectively, onto a regular grid of $1.875^{\circ} \times 1.875^{\circ}$ latitude-longitude resolutions. This resolution was chosen to allow comparison with previous work using the CPTEC/COLA GCM, which used a corresponding resolution in the spectral form. The score was computed on every grid-box, which contained at least one observation.

[34] Scores were calculated over 4 regions (Figure 9): whole South America (SA); northern region (NO) within 15.5°S to 14.5°N and 90°W to 45°W ; northeastern region (NE) within 15.5°S to 14.5°N and 45°W to 25.5°W ; and central-southern region (CS) within 50°S to 15.5°S and 90°W to 25.5°W . These regions were chosen according to the approximate area of distinct and prevailing weather systems.

[35] Figure 10a shows the ETS and the BIAS for August 1997. The rain/no-rain category, corresponding to the threshold 9 mm, is well simulated by the model. ETS attains values of about 0.5 for this threshold. The score decreases slowly toward higher rainfall rates. The CS region shows the highest scores, and the NE region, the smallest ones. The BIAS score shows that precipitation is generally overestimated, except over NE. At higher thresholds, precipitation overestimate tend to increase. However, at those thresholds, the number of observations decrease and the scores have smaller significance.

[36] During November 1997 (Figure 10b), the wet month, the ETS increases considerably at most of the precipitation thresholds, and the BIAS is generally closer to 1. A sharp change on the simulation quality occurs between the thresholds 100 and 200 mm, in which the ETS drops and the BIAS increases. This occurs with a significant reduction in the number of observations. Similar to the August case, the CS region has the highest scores and NE, the lowest ones. The larger number of precipitation events during this month gives confidence on this model behavior. These scores are

much higher than daily precipitation forecast evaluation such as done by *Chou and Justi da Silva* [1999]. In their work, ETS and BIAS of the daily precipitation forecasts from the operational 40-km Eta/bucket model were estimated for a 1-year period. These scores were higher over the Center-South region of South America where frontal passages predominate. In the total monthly precipitation, the daily variability is not taken into account for score computation. Daily evaluation would strongly penalize the limited area models during long-term integrations because of the reduced predictability in higher resolution. A regional model, which is periodically reinitialized during extended integrations, may capture the daily variations more accurately. Nevertheless, the results from this evaluation show some similarities to those obtained by *Chou and Justi da Silva* [1999]. In that work, short-range forecasts over South America using the Eta model with the bucket scheme also produced precipitation scores for CS region higher than for the other regions, whereas the NE region had the smallest skill (their Figure 2).

3.3. Surface Temperature

[37] In the dry month simulation, the surface temperature over Brazil showed good agreement with observations. The August 1997 mean observed temperature and the model air temperature at canopy level are shown in Figures 11a and 11b, respectively. The available near-surface temperature data for verification is the observed mean temperature. This temperature is computed from: (equation (2)) $T_{00} + T_{\max} + T_{\min} + T_{12})/5$, where T_{00} and T_{12} are shelter temperatures at 0000 and 1200 UTC, respectively, and T_{\max} and T_{\min} are the maximum and minimum temperatures of the day, respectively. Comparison needs to be based on contour patterns rather than absolute values. However, it should be reminded

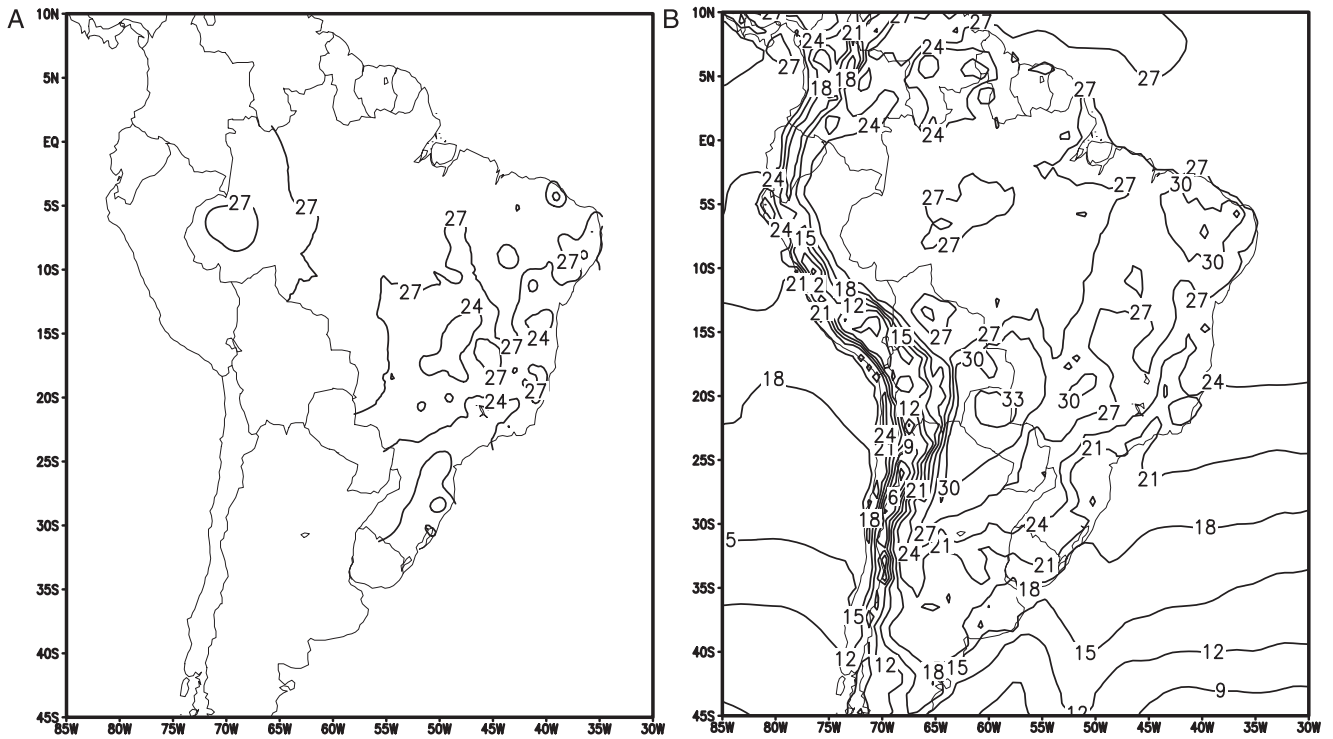


Figure 12. Same as Figure 11, except for November 1997.

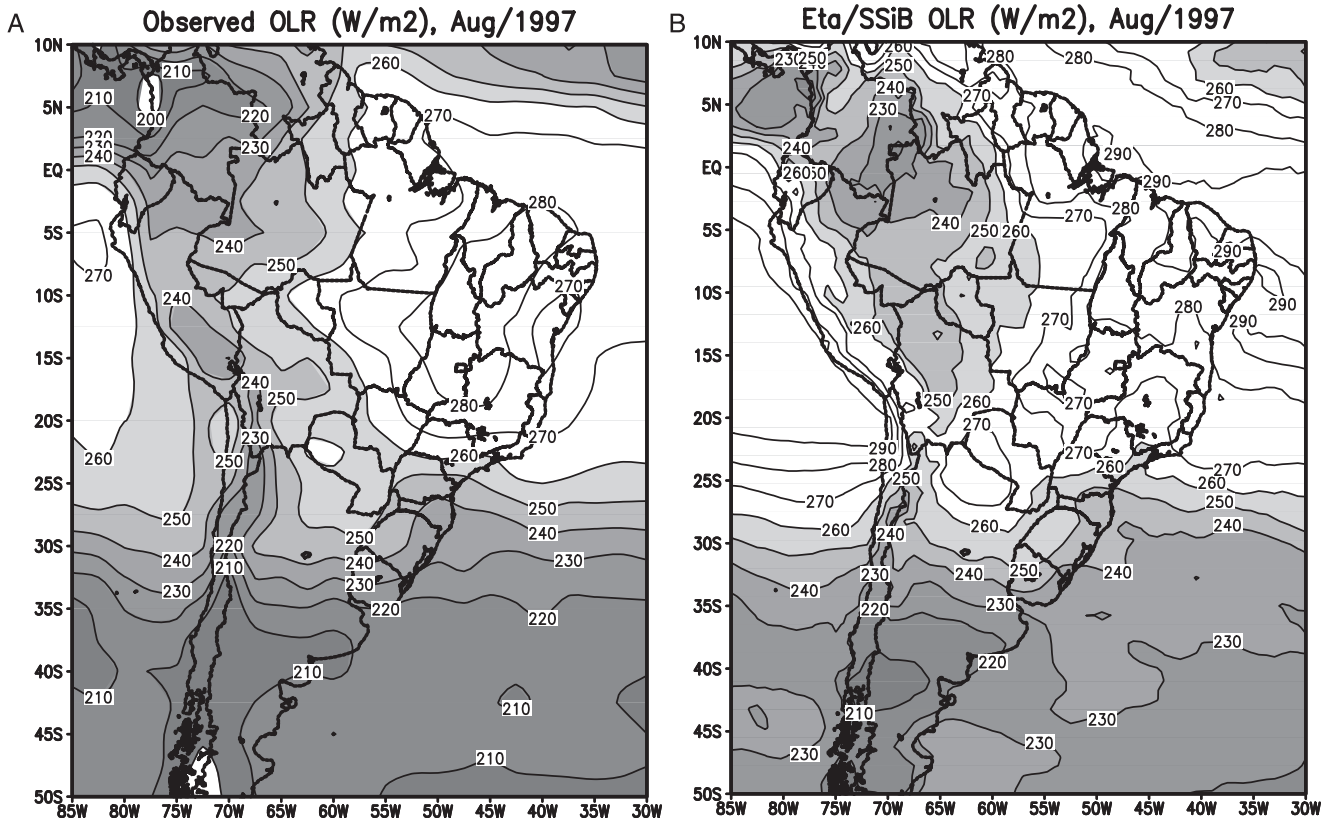


Figure 13. August 1997 mean outgoing longwave radiation ($W m^{-2}$): (a) Data provided by the NOAA-CIRES Climate Diagnostics Center, Boulder, CO, from their Web site at <http://www.cdc.noaa.gov/> and (b) Eta/SSiB simulation.

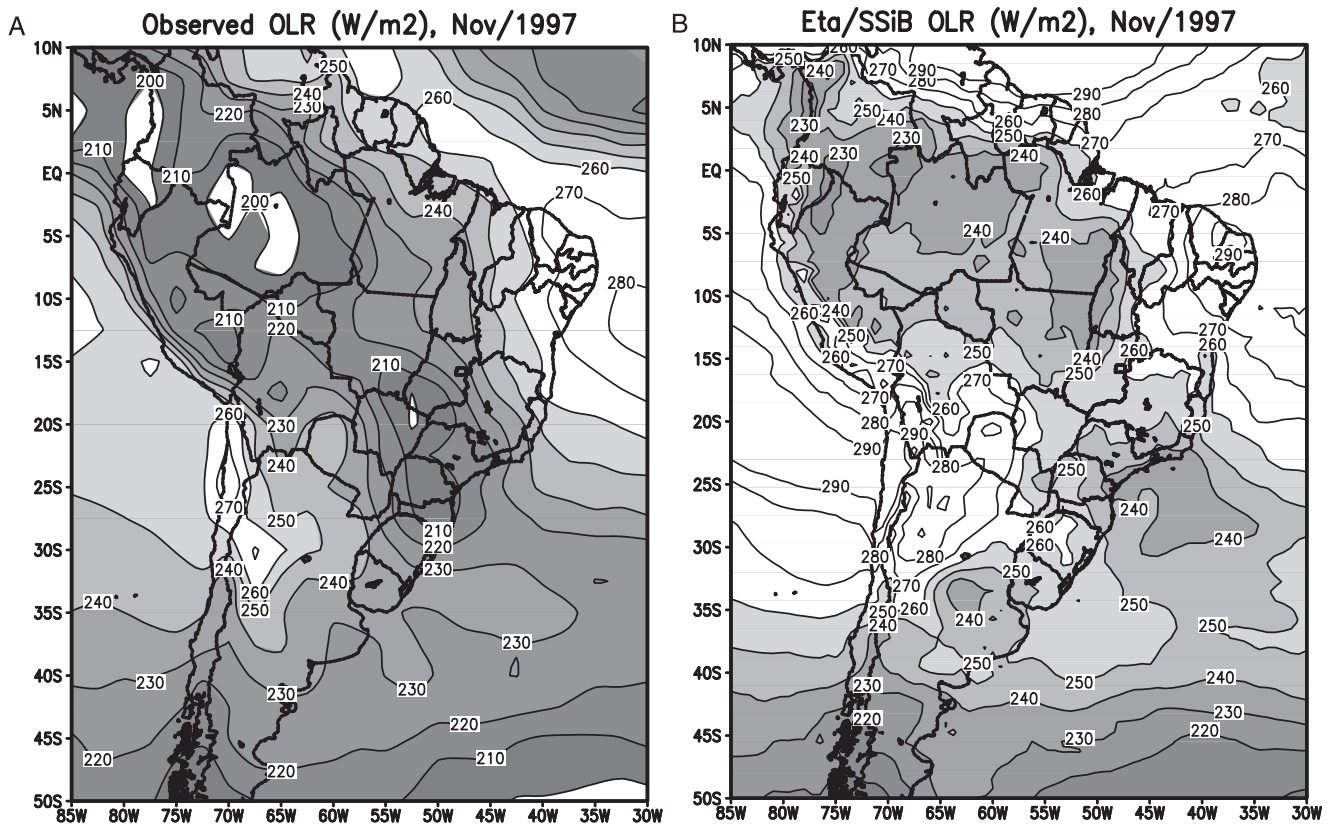


Figure 14. Same as Figure 13, except for November 1997.

that the air temperature at the canopy height is different from the temperature in a grassland site. For example, the model canopy height in the Amazon rain forest is set to 35 m. Therefore, the model canopy air temperature is expected to be smaller than the observed temperature. A simple interpolation to the same height would not improve the comparison between the modeled and observed surface temperature over the Amazon.

[38] Both fields in Figure 11 show the contrast between the relatively warmer tropical and the colder subtropical air masses, as well as the cooler temperatures in a band along the Brazilian eastern coast. The largest differences are of the order of 3°C . These are observed in extreme northern Brazil, and in the eastern Amazon region, around 55°W and 5°S , where model temperatures are colder than observations; and over central Brazil, around 55°W and 17°S , where the model temperature is warmer, favoring convective instability over this region. The spatial correlation between the model canopy air temperature and the observed mean temperature during August 1997 is 0.77.

[39] November 1997 mean temperature fields are presented in Figure 12. It shows that the model can also simulate patterns and magnitudes close to observations with differences up to 3°C . The model air temperature at canopy level in the Amazon region is smaller than observed mean temperatures, partially due to the high rain forest trees. This results in a spatial correlation between the model canopy air temperature and the observed mean temperature of 0.54 during November 1997.

[40] During the dry month, warmer temperatures were simulated in a northeast-southwest band extending from

Northeast Brazil to the South, whereas during the wet month model temperatures are warmer than observations over the Central and extreme Northeast Brazil. These maximum of temperatures seem to be a feature of coupled atmospheric-SSiB models since it is also found in the CPTEC/COLA GCM run of the same case, which will be discussed in section 4. The higher model surface temperatures were partly caused by an excess of incoming short-wave radiation at the surface under clear sky conditions.

3.4. Outgoing Longwave Radiation

[41] Figure 13 shows the outgoing longwave radiation (OLR) observed during August 1997 [Liebmann and Smith, 1996]. This data set was obtained from twice daily advanced very high resolution radiometer (AVHRR) soundings from the American National Oceanic and Atmospheric Administration (NOAA) polar-orbiting satellite, and averaged over the month. For the studied period, the available data was constructed from one daily passage at 1430 LST. Because of differences in the derivation of OLR between model and observations, model validation will be based mostly on the patterns.

[42] The simulated OLR pattern resembles the observed one. Lower values are found in the midlatitudes and along the western side of the continent, following the Andes Cordillera and reaching a minimum over Colombia. However, the model shows an overestimate of OLR by at least 10 W m^{-2} . Large positive biases, of about 40 W m^{-2} and 20 W m^{-2} , can be found off the coast of Peru, and to the north of the equator, respectively. These are cloud-free regions in the model simulations. During the wet month, the positive bias of

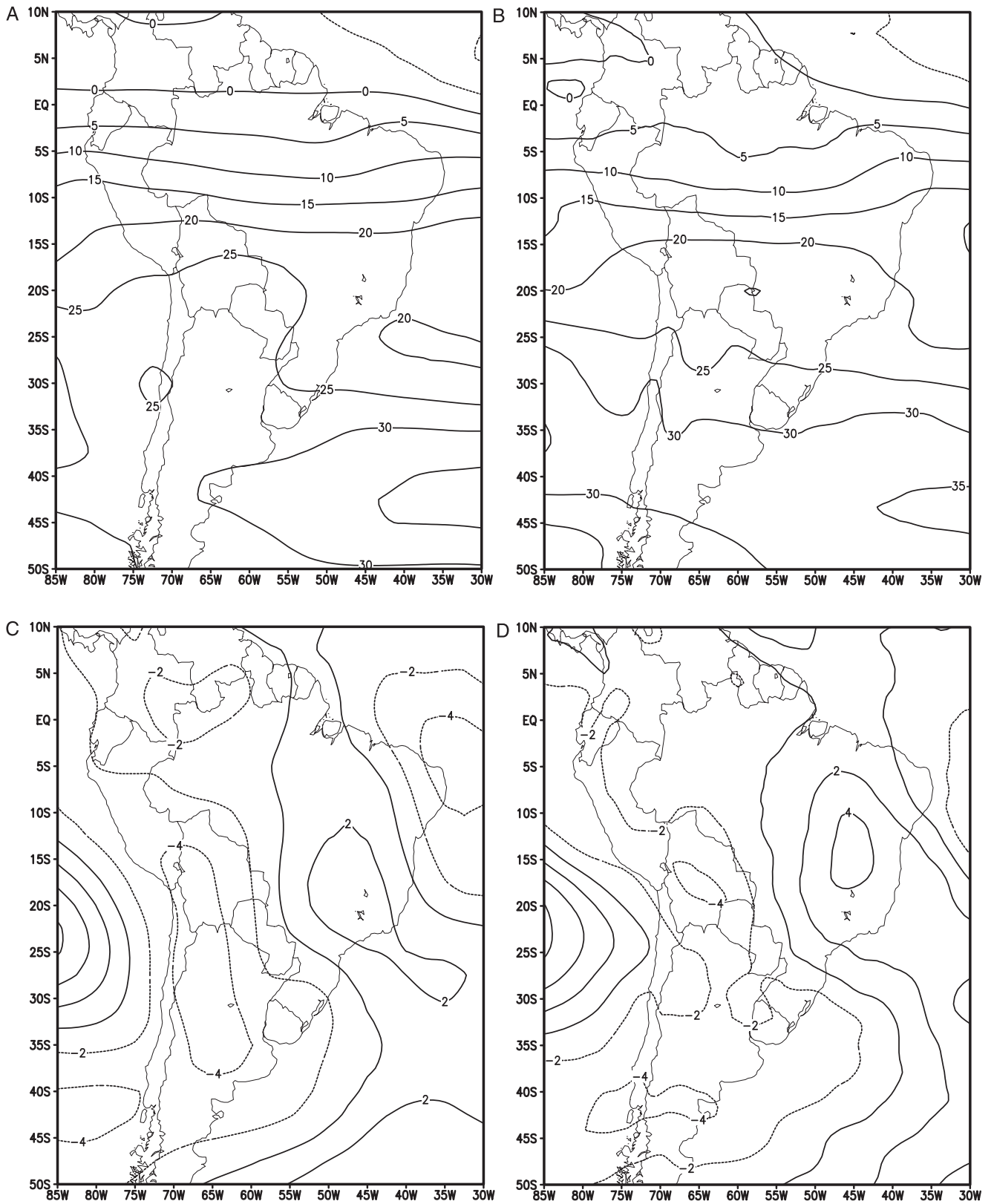


Figure 15. August 1997 winds (m s^{-1}): zonal component (a) NCEP reanalysis and (b) Eta/SSiB simulation; meridional component (c) NCEP reanalysis and (d) Eta/SSiB simulation.

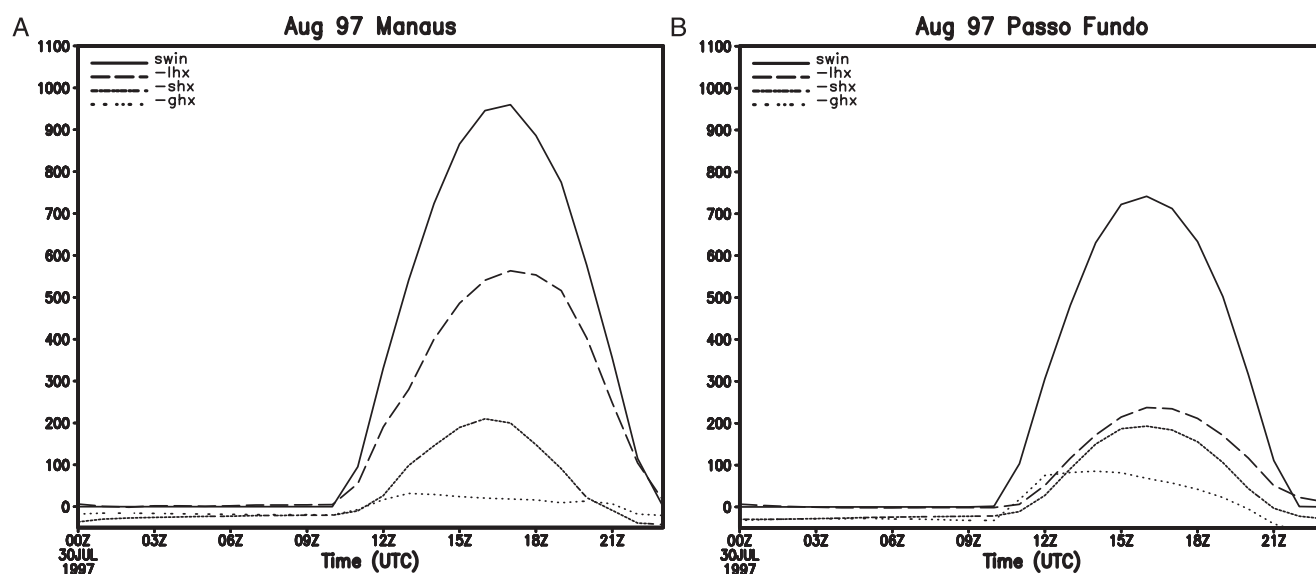


Figure 17. August 1997 diurnal cycle of surface energy fluxes (W m^{-2}): (a) near a tropical station, Manaus, and (b) near a subtropical area, Passo Fundo. Solid line refers to incoming shortwave radiation, long dashed line refers to latent heat flux, short-dashed line refers to sensible heat flux, and dotted line refers to ground heat flux.

[43] The positive bias in the whole domain may be associated with the excess of energy input to the system. The preference of those maximum bias regions for areas of deep convection suggests that the convective parameterization scheme may not produce convective clouds with sufficiently high tops, or temperatures at cloud top levels are too high. Along the coast of Peru, maximum OLR is simulated to the south over the Pacific Ocean. This region is often covered by a shallow layer of stratocumulus clouds produced over the cold Peru current. The model simulation hardly produces these clouds, and consequently more incoming solar radiation reaches the surface. Stratiform clouds are formed explicitly in the model, however, adjustments in the model parameters seem to be needed to correct this type of cloud formation.

3.5. 250-hPa Mean Winds

[44] Validation of the large-scale features of the simulation is carried out with 250-hPa monthly mean winds. NCEP reanalysis data, at $2.5^\circ \times 2.5^\circ$ latitude-longitude resolution, are used for comparison with model output. These data were accessed from the site <http://www.cdc.noaa.gov/>. Figure 15 shows the zonal and meridional winds from NCEP-NCAR (National Center for Atmospheric Research) reanalyses and simulation during August 1997. The magnitude and general pattern of the zonal wind are similar in the reanalyses and simulation. Zonal winds range from about -5 m s^{-1} to 35 m s^{-1} , from the northern boundary to the southern boundary in both data. However, easterlies prevail along the latitudes between the equator and 10°N in the reanalysis, whereas the simulated easterlies do not penetrate into the continent. Midlatitude westerlies are slightly stronger in the simulation than in the reanalyses.

[45] The analyzed and simulated wave pattern of the meridional wind component (Figures 15c and 15d) are in phase. Northerlies occur in the western half of the continent

and in the northeastern corner of Brazil, however, they are underestimated.

[46] During November 1997, the 250-hPa zonal winds were maximum at about 35°S and minimum over the central part of Brazil (Figure 16a). The simulation (Figure 16b) captured correctly the position and shape of these two extreme values, however easterlies over central Brazil were stronger in the simulation. The shear zone between tropics and subtropics is reproduced by the model. This zone is located in the southern flank of the anticyclone, which resulted from large-scale convection. The shear is stronger in November than August 1997. *Tanajura* [1996] showed that these winds are in thermal wind balance during the summer season. The meridional component shows maxima and minima oriented in the northwest-southeast direction (Figure 16c), with southerlies over the central part of the continent, and northerlies over Argentina. These northerlies are underestimated by the model (Figure 16d). This wind configuration produces a vortex over the coast of Northeast Brazil. This vortex is more inland in the observations.

[47] In summary, during the wet month the model tend to have an easterly bias, which is not so clear in the dry month. The northerlies are weakly simulated in both months. Overall the errors showed small magnitudes and the large scale can be considered well simulated.

3.6. Diurnal Cycle

[48] Many climatic features over tropical South America, such as the intense convective activity in Amazon, have strong diurnal variation. Indeed, climate is the result of the interactions of phenomena with various timescales. A model, which can resolve higher frequency phenomena correctly, will be able to simulate climate more accurately. The simulation of the mean diurnal variation of some quantities that impact over the South American climate is presented in this subsection.

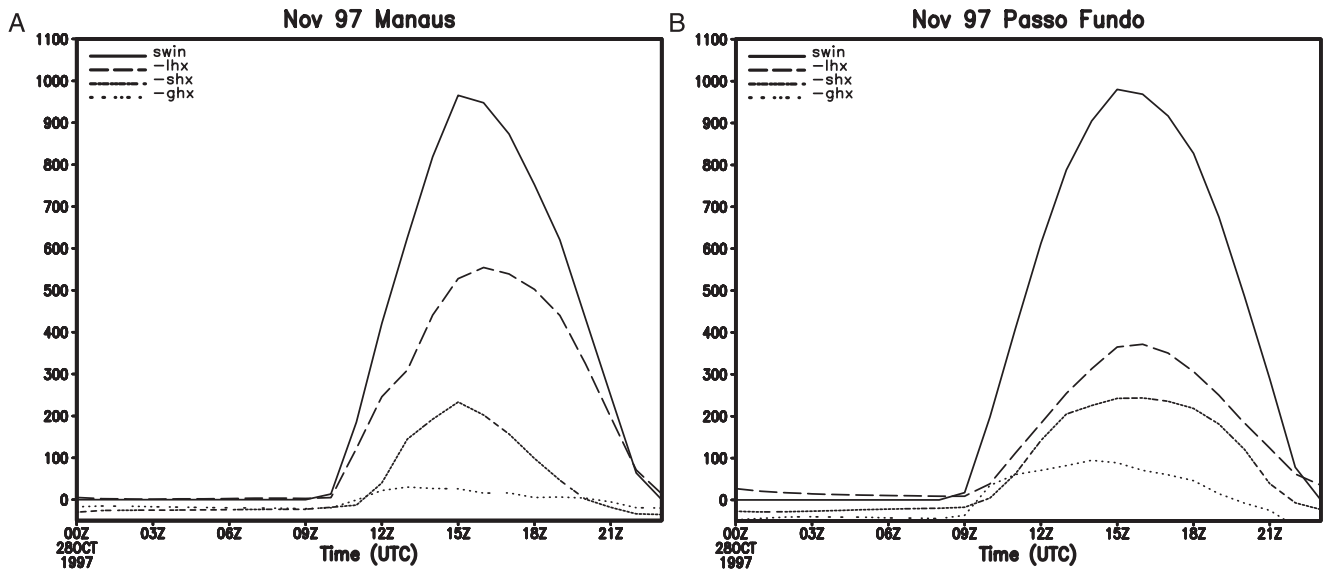


Figure 18. Same as Figure 17, except for November 1997.

[49] Figures 17a and 17b show the simulated mean diurnal cycle of surface incoming shortwave radiation, latent heat, sensible heat and ground heat fluxes during August 1997 over two model grid-boxes. The values shown in these figures were derived from hourly model outputs. The sites were taken to illustrate the simulated surface fluxes at two contrasting land-cover types: one near Manaus, at $2.5^{\circ}S$ and $60^{\circ}W$, which is in the tropical rain forest region (see vegetation map in Figure 1); and the other near Passo Fundo, at $28.15^{\circ}S$ and $52.24^{\circ}W$, which is in a cultivation region.

[50] Near Manaus, the incoming shortwave radiation at the surface starts increasing around 1000 UTC and attains its maximum, about $950 W m^{-2}$, around 1600–1700 UTC. Near Passo Fundo, this variable attains its maximum, about $750 W m^{-2}$, at around 1600 UTC. The different longitudes of the sites result in different timing of the maximum incoming shortwave radiation during this time of the year, and consequently affect the phase of the other energy fluxes too.

[51] The peaks of the simulated latent and sensible heat fluxes also occur around 1600–1700 UTC, which agrees with the observational data from the Anglo-Brazilian Amazonian Climate Observation Study (ABRACOS) [Gash *et al.*, 1996] conducted from 4 October to 2 November 1990 and from 29 June to 10 September 1991 [Xue *et al.*, 1996]. The ground heat fluxes peak around 1300 UTC, which is about 2 to 3 hours earlier than the peaks observed during ABRACOS. This model behavior was also identified in off-line simulations of SSiB, and it was attributed to the assumption of periodic forcing in the force-restore method used to calculate surface temperature in SSiB [Xue *et al.*, 1996].

[52] When compared with ABRACOS data magnitude, the model overestimates the surface latent heat fluxes. The mean diurnal cycle observed in the experiment during the 1991 ABRACOS campaign showed maximum values of about $300 W m^{-2}$, while the model results peak at about $550 W m^{-2}$. Another observational data set from the Rondônia Boundary Layer Experiment carried out in July 1993 and August 1994 showed the maxima in the rain forest

site at Ji-Paraná, Rondônia, of about $350 W m^{-2}$ [Silva, 1998]. These two data sets confirm the model positive bias in the surface latent heat fluxes. The surface sensible heat flux is also overestimated by the model. Values observed during ABRACOS campaign show maximum of about $100 W m^{-2}$ while model produces maximum of about $200 W m^{-2}$. On the other hand, the magnitude of the ground heat fluxes agree well with ABRACOS data.

[53] The major differences between the surface fluxes at the Manaus and Passo Fundo sites are the incoming shortwave radiation and the latent heat flux. There is an incoming shortwave radiation difference between the two sites of about $200 W m^{-2}$, which is caused by their latitudinal distance. The latent heat flux difference of about $300 W m^{-2}$ can be explained by the different vegetation cover, energy input, and soil moisture availability. The surface sensible heat fluxes do not vary substantially from one site to the other. Consequently, distinct model Bowen ratios at the rain forest and the cultivation sites are obtained.

[54] Figures 18a and 18b show the same variables as in Figures 17a and 17b, but for November 1997. During this wet month, the peaks of the simulated incoming shortwave radiation at the surface in the Manaus and Passo Fundo sites show the same intensity, about $950 W m^{-2}$, differently from August. The peaks occur around 1500 UTC, which is about one hour earlier than in August. This affects the other surface fluxes which also tend to shift their peaks one hour earlier with respect to the August simulation. The simulated diurnal variation of surface fluxes at Manaus in November are similar to the fluxes in August. However, at Passo Fundo there is an increase of incoming shortwave radiation as a response to seasonal variation. This increase is accompanied by increases in the other surface fluxes. The ground heat flux peak was shifted to about 1400 UTC, in both sites.

[55] The model has the energy surface fluxes in balance. However, the excess of the atmospheric model incoming shortwave radiation at the surface is partitioned mostly between the sensible and, mainly, the latent heat fluxes. The SSiB model behaves similarly to its offline version,

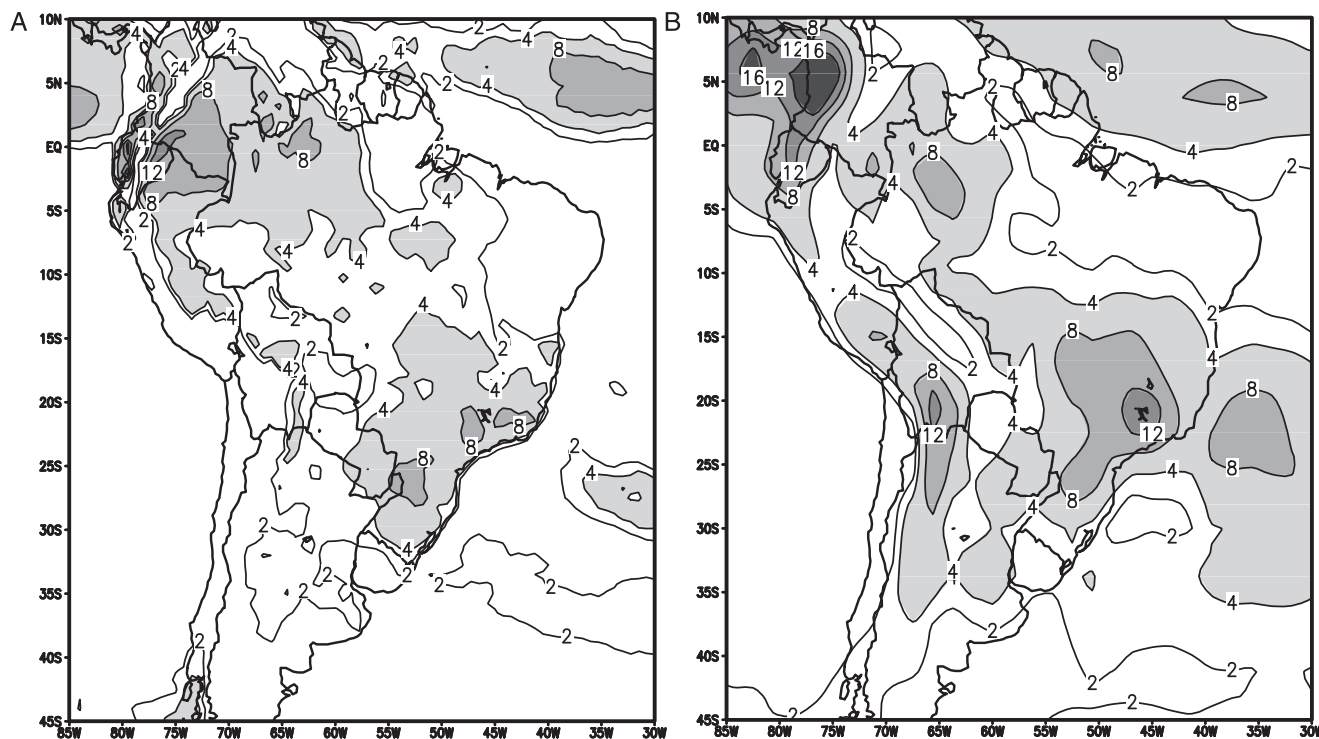


Figure 19. November 1997 mean precipitation (mm d^{-1}) from (a) Eta/bucket run and (b) CPTEC/ COLA GCM run. Adapted from *Chou et al.*'s [2000] study.

but cannot cope with the errors in the atmospheric model component.

4. Comparison with Eta/ Bucket and GCM

[56] Model stability in long-term integrations was also assessed by *Chou et al.* [2000] using the Eta with bucket hydrology model. The same periods, August and November 1997, were used in the integrations. CPTEC/COLA GCM was integrated to provide boundary conditions for the Eta model. This allows comparison of the current integrations with the Eta/bucket version and the GCM runs.

[57] During the dry month, the Eta/SSiB simulated the major precipitation (Figure 2) regions similarly to the Eta/ bucket, except for the precipitation along the eastern coast of Northeast Brazil, which is missing in the Eta/SSiB. Generally higher precipitation rate is produced by Eta/SSiB in the Amazon region. During the wet month, Eta/SSiB produces higher precipitation amounts over the central part of the continent (Figure 4), and closer to the observations than the Eta/bucket (Figure 19a). The global model run for this month (Figure 19b) also produced higher amounts than Eta/bucket. Precipitation scores from Eta/SSiB are comparable to Eta/bucket, except over Northeast Brazil, where the SSiB tend to overestimate at higher thresholds and the bucket underestimates in all thresholds in both dry and wet months. However, an interesting result is that the score, particularly the bias score, produced by the Eta/SSiB during the wet month is similar to the global model, which also uses SSiB model. During the wet month, when most precipitation is concentrated in the CS region, the Eta/SSiB produced slightly better equitable threat score at thresholds above 100 mm.

[58] Eta/SSiB canopy air temperature (Figures 11 and 12) tend to be warmer than the Eta/bucket surface temperature (Figures 7a and 11b in *Chou et al.*'s [2000] study) over Northeast Brazil and slightly warmer over the Amazon region in both dry and wet months. In the Amazon region, the Eta/bucket underestimated the temperatures, whereas the Eta/SSiB introduced some correction. Similarly, the comparison was based on the pattern of the contours. The Eta/SSiB maximum temperatures over Northeast Brazil are similar to the GCM/SSiB, in shape and position, in both months. In August 1997, the maximum was elongated and oriented in a southwest-northeast direction, whereas in November, it has more circular shape and approaches the eastern coast.

[59] During August 1997, the excessive OLR found over the northwestern part of the continent in the Eta/bucket version is clearly reduced in the Eta/SSiB (Figures 13 and 14). During November 1997, the large-scale NW-SE oriented band related to a moisture convergence zone is hardly seen in the Eta/bucket (Figure 12b in *Chou et al.*'s [2000] study), however, it is improved in the Eta/SSiB. The positive bias of OLR over the Pacific near the coast of Peru

Table 1. Mean Fluxes Over South America for August 1997

Fluxes	Eta/SSiB	Eta/Bucket
precipitation (mm d^{-1})	2.76	1.74
sfc latent heat flux (W m^{-2})	88.47	69.36
sfc sensible heat flux (W m^{-2})	57.44	43.01
sfc incoming shortwave radiation (W m^{-2})	271.18	276.70
sfc incoming longwave radiation (W m^{-2})	345.66	336.70
sfc outgoing shortwave radiation (W m^{-2})	62.80	59.04
sfc outgoing longwave radiation (W m^{-2})	425.33	415.08

Table 2. Mean Fluxes over South America for November 1997

Fluxes	Eta/SSiB	Eta/Bucket
precipitation (mm d^{-1})	4.77	3.24
sfc latent heat flux (W m^{-2})	114.34	99.25
sfc sensible heat flux (W m^{-2})	71.76	44.18
sfc incoming shortwave radiation (W m^{-2})	321.74	328.66
sfc incoming longwave radiation (W m^{-2})	363.98	356.97
sfc outgoing shortwave radiation (W m^{-2})	73.51	72.13
sfc outgoing longwave radiation (W m^{-2})	443.66	430.97

and Chile is, however, larger in the SSiB. This version seems to have improved OLR over the land areas with cloud cover, however, over the ocean, in cloud-free regions, this version maintains the overestimate.

[60] Tables 1 and 2 contain monthly mean area averaged precipitation, and surface fluxes of latent heat, sensible heat, incoming and outgoing shortwave radiation, for August and November 1997, respectively, produced by the Eta/SSiB and the Eta/bucket models. These quantities were averaged over South America land points. The results show that in both months the Eta/SSiB has larger precipitation than the Eta/bucket. This is partly due to the larger latent heat fluxes. Despite this, the Eta/SSiB near surface temperatures are higher than observations, in agreement with high sensible heat fluxes. Both models have similar incoming surface radiation, however, the excess of incoming shortwave radiation in the Eta/bucket is larger. This is consistent with larger OLR shown in previous section. The magnitude of the residue of these fluxes at the surface is much larger in the Eta/bucket, and may be responsible for the lower near surface temperatures. On the other hand, the Eta/SSiB high near surface temperature is not compensated by the ground heat.

5. Sensitivity Runs

[61] To further investigate the Eta/SSiB model performance, a series of five 1-month independent integrations were used to test model sensitivity on lateral boundary conditions, initial condition and model physics. It is known that there is a strong control of the lateral boundary conditions on the regional model solutions [Sass and Christensen, 1995]. However, as shown by Weisse *et al.* [2000] through an ensemble study, the internal variability of regional models may have strong influence on the model solution and mask changes in the surface boundary conditions. This section presents an ensemble of 1-month integrations to investigate the robustness of the November 1997 integration.

[62] The integration initialized on 00Z 29 October 1997, and discussed in the previous sections, is referred to as the control run. In the other runs, from runs 2 to 5, initial condition (IC), sea surface temperature (SST), lateral bound-

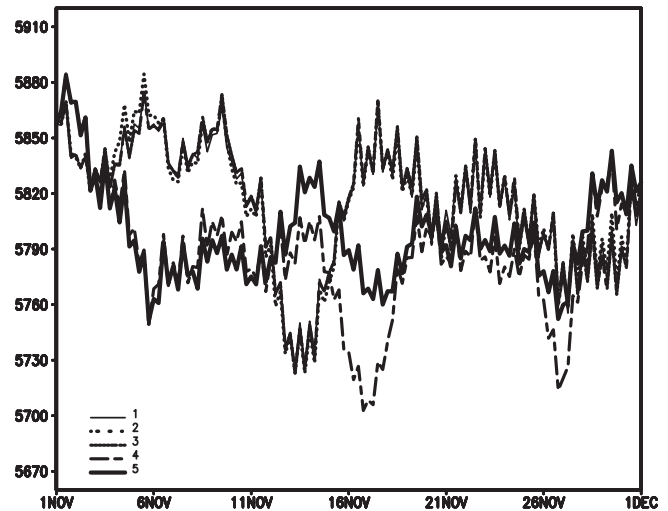


Figure 20. 500-hPa geopotential height (m), averaged over the subtropical region for five Eta model runs for November 1997. See Table 3 for summary of the runs.

dary condition (LBC), and land surface model physics were altered. In the run 2, the initial condition started one day before the control run, i.e., on 00Z 28 October 1997. In the run 3, the lower boundary was changed by substituting the observed SST on 1 November, for the November 1997 mean SST. In the run 4, the lateral boundary conditions were changed to CPTEC/COLA GCM 1-month forecasts. In the run 5, the model used a different land surface physics. Assuming that these runs result from perturbations applied to the initial, lateral and lower boundary conditions, and in model internal physics, these runs could be considered as an ensemble run. Table 3 summarizes the model setups for these five runs.

[63] The 500-hPa geopotential height averaged over the subtropical region, defined in Figure 6, is shown in Figure 20. One can notice that the control run evolves closely to the runs that had SST and the IC changed. These three runs had in common the lateral boundary conditions. The other two runs, 4 and 5, which used the CPTEC/COLA GCM forecasts as lateral boundary conditions, show similarities up to day 12 November. From that day onwards, the curves tend to depart from each other. Three separate curves, whose runs differ by the lateral boundary conditions and the land-surface scheme, can be distinguished from that figure.

[64] Although the changes in the geopotential height as well as in other fields were very small in the area average sense, differences in the spatial distribution were observed among the ensemble members. For instance, Figure 21 shows the difference between the November 1997 precipitation produced by the control run and the mean of the five

Table 3. Summary of the Ensemble Experiment During November 1997

Run	Lateral boundary	Initial date	SST	Land surface
1 control	NCEP analysis	00Z 29 October 1997	1 November 1997	SSiB
2 IC	NCEP analysis	00Z 28 October 1997	1 November 1997	SSiB
3 SST	NCEP analysis	00Z 29 October 1997	November 1997 mean	SSiB
4 LBC	GCM forecast	00Z 1 November 1997	1 November 1997	SSiB
5 physics	GCM forecast	00Z 1 November 1997	1 November 1997	bucket

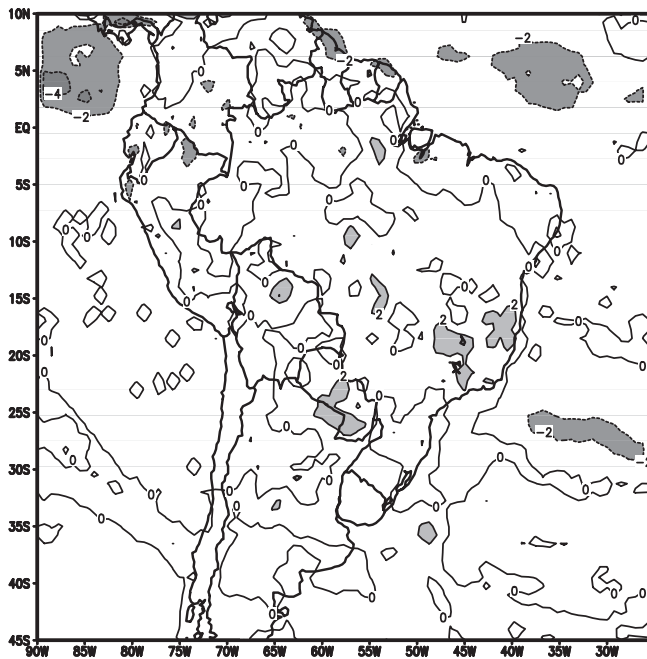


Figure 21. Difference between the November 1997 precipitation (mm d^{-1}) produced by the control run and the mean of the five-member ensemble.

ensemble members. The magnitude of these differences ranges from -4 mm d^{-1} to 2 mm d^{-1} . When members with the same lateral boundary conditions are used, the magnitude of those differences ranges from -2 mm d^{-1} to 2 mm d^{-1} . This indicates that the lateral boundary conditions are controlling the magnitude of the model variability. Surface temperature differences of about 2°C were also found in regions of southeastern and southern Brazil.

[65] Therefore, in agreement with other studies, e.g., *Sass and Christensen* [1995], *Weisse et al.* [2000], *Laprise et al.* [2000], the results from the ensemble experiment show that the lateral boundary conditions and the model internal physics are the most important factors to control limited area model long-term integrations and large-scale predictability. However, the ensemble technique applied to regional climate models are useful to provide statistical and predictability information at small scales.

6. Summary and Conclusions

[66] The Eta model coupled with SSiB scheme is configured to run over South America on a 80-km resolution. One-month continuous integrations for wet and dry season months were carried out. Lateral boundaries were provided by NCEP analyses and simulations were evaluated against available observations, such as precipitation, temperature and OLR. Monthly mean of these variables compared well with model simulations during the dry month. During the wet month, simulated precipitation area was broader and induced subsidence over the ITCZ, inhibiting part of its convective band. Temperatures compared well with observation, but they were slightly cooler over the Amazon and warmer over Northeast Brazil regions in both months. OLR showed generally some positive bias, particularly over adjacent oceans, but posi-

tioned correctly areas of minimum and maximum values. According to upper level winds, large-scale features such as jets and waves were well simulated.

[67] The daily variability of the model was assessed over two small regions, a tropical and a subtropical. During the dry month, the simulated precipitation variability followed reasonably the observations. However, during the wet month, the simulations showed reduced quality.

[68] The model reproduced the major characteristics of the diurnal cycle of surface fluxes at a rain forest grid point located in the tropics, and a cultivation grid point in the subtropics. The peaks occurred at the correct time, but the fluxes tend to be overestimated, particularly the latent heat flux. This positive bias in the fluxes may have caused the lower surface temperatures over the Amazon. A common problem in numerical atmospheric radiation models is the excess of the incoming shortwave radiation at the surface due to deficient extinction by water vapor and aerosols, and errors in cloud treatment. This radiative problem was also found in the Eta model in the present and in other investigations [*Hinkelman*, 2000]. The high values of surface latent and sensible heat fluxes produced by the Eta/SSiB model were a response to excessive incoming shortwave radiation at the surface. A fair model validation of its surface fluxes would require either a previous correction in the atmospheric radiation scheme or a retuning of the SSiB scheme parameters. The second alternative may depart the parameters from more realistic values and may conceal the errors produced by the other components of the model.

[69] Comparison of these results with a version of the model using bucket scheme and CPTEC/COLA GCM integrations performed by *Chou et al.* [2000] showed that the Eta/SSiB simulations had features similar to the GCM, which is also coupled with SSiB. Positive bias at larger precipitation rates and over Northeast Brazil, and warmer temperatures over the Amazon and Northeast Brazil were produced by both current coupled Eta/SSiB and GCM/SSiB model simulations. Therefore, some simulated features seem to be related to SSiB physics and a fine tuning seems to be necessary in both Eta and GCM coupled with SSiB. OLR positive bias over deep convective areas were reduced in the Eta/SSiB integrations compared to Eta/bucket.

[70] The model performance dependence on factors such as lateral boundary conditions, initial conditions, lower boundary conditions through SST, and internal physics was assessed through sensitivity experiments. The results showed that the lateral boundary conditions exert strong control on the simulation. The adjustment between model physics and lateral boundary forcing drifts the solution to different atmospheric states. This introduces a difficulty in the derivation of the limited area model climatology for future climate forecast purposes. A climatology produced from a regional model may vary depending on the analyses or GCM forecast data sets used as lateral boundaries.

[71] Evaluation or correction of the vegetation map over Brazil is being carried out using Brazilian data set, in an attempt to produce detailed quality control. Tests with higher horizontal resolution Eta/SSiB model are being performed to verify the influence of the improved surface characteristics on mesoscale circulations. Recent observations collected over the Amazon region during the 1999

WET-LBA campaign will be used to further validate the Eta/SSiB model.

[72] **Acknowledgments.** The authors would like to thank the South America vegetation map prepared by M. C. Hansen and collaborators of University of Maryland at College Park. This work was funded by LBA/NASA grant NRA98-MTPE-01 and Fundação de Amparo à Pesquisa do Estado de São Paulo (FAPESP) grant 97/11007-1.

References

- Betts, A. K., and M. Miller, A new convective adjustment scheme, part II, Single column model tests using GATE wave, Bomex and arctic air-mass data sets, *Q. J. R. Meteorol. Soc.*, **112**, 693–709, 1986.
- Black, T. L., New NMC mesoscale eta model: Description and forecast examples, *Weather Forecast.*, **9**, 265–278, 1994.
- Bonatti, J. P., CPTEC atmospheric general circulation model (in Portuguese), in *Climanálise*, Especial Edition, Inst. Nac. de Pesqui. Espaciais, Cachoeira Paulista, Brazil, 1996.
- Chou, S. C., and M. G. A. Justo da Silva, Evaluation of the Eta model precipitation forecasts over South America, in *Climanálise*, vol. 14, Inst. Nac. de Pesqui. Espaciais, Cachoeira Paulista, Brazil, 1999.
- Chou, S. C., A. M. B. Nunes, and I. F. A. Cavalcanti, Extended forecasts over South America using the regional eta model, *J. Geophys. Res.*, **105**, 10,147–10,160, 2000.
- Dickinson, R. E., R. M. Errico, F. Giorgi, and G. T. Bates, A regional climate model for the western United States, *Clim. Change*, **15**, 383–422, 1989.
- Dorman, J. L., and P. J. Sellers, A global climatology of albedo roughness length and stomatal resistance for atmospheric general circulation models as represented by the Simple Biosphere Model (SiB), *J. Appl. Meteorol.*, **28**, 833–855, 1989.
- Fels, S. B., and M. D. Schwarzkopf, The simplified exchange approximation: A new method for radiative transfer calculations, *J. Atmos. Sci.*, **32**, 1475–1488, 1975.
- Fennessy, M., and J. Shukla, Seasonal prediction over North America with a regional model nested in a global model, *J. Clim.*, **13**, 2605–2627, 2000.
- Figueroa, S. N., and C. A. Nobre, Precipitation distribution over central and western tropical South America, *Climanálise*, 36–45, 1990.
- Figueroa, S. N., P. Satyamurty, and P. L. Silva Dias, Simulations of the summer circulation over the South American region with an eta coordinate model, *J. Atmos. Sci.*, **52**, 1573–1584, 1995.
- Gash, J. H. C., C. A. Nobre, J. M. Roberts, and R. L. Victoria (Eds.), *Amazonian Deforestation and Climate*, 611 pp., John Wiley, New York, 1996.
- Giorgi, F., On the simulation regional climate using a limited area model nested in a general circulation model, *J. Clim.*, **3**, 941–963, 1990.
- Giorgi, F., and G. T. Bates, The climatological skill of a regional model over complex terrain, *Mon. Weather Rev.*, **117**, 2325–2347, 1989.
- Giorgi, F., and L. O. Mearns, Introduction to special section: Regional climate modeling revisited, *J. Geophys. Res.*, **104**, 6335–6352, 1999.
- Hansen, M. C., R. S. DeFries, J. R. G. Townshend, and R. Sohlberg, Global land cover classification at 1-km spatial resolution using a classification tree approach, *Int. J. Remote Sens.*, **21**, 1331–1364, 2000.
- Hinkelmann, L., *International Radiation Symposium IRS 2000: Current Problems in Atmospheric Radiation*, Abstracts, 24–29 July 2000, p. 116, St. Petersburg State Univ., St. Petersburg, Russia, 2000.
- Horel, J. D., A. N. Hahmann, and J. E. Geisler, An investigation of the annual cycle of the convective activity over the Tropical Americas, *J. Clim.*, **2**, 1388–1403, 1989.
- Janjić, Z. I., Forward-backward scheme modified to prevent two-grid-interval noise and its application in sigma coordinate models, *Contrib. Atmos. Phys.*, **52**, 69–84, 1979.
- Janjić, Z. I., Nonlinear advection schemes and energy cascade on semi-staggered grids, *Mon. Weather Rev.*, **112**, 1234–1245, 1984.
- Janjić, Z. I., The step-mountain coordinate: Further developments of the convection, viscous sub-layer, and turbulence closure schemes, *Mon. Weather Rev.*, **122**, 927–945, 1994.
- Ji, Y., and A. D. Vernekar, Simulation of the Asian summer monsoons of 1987 and 1988 with a regional model nested in a global GCM, *J. Clim.*, **10**, 1965–1979, 1997.
- Lacis, A. A., and J. E. Hansen, A parameterization of the absorption of solar radiation in the earth's atmosphere, *J. Atmos. Sci.*, **31**, 118–133, 1974.
- Laprise, R., M. R. Varma, B. Denis, D. Caya, and I. Zawadzki, Predictability of a nested limited-area model, *Mon. Weather Rev.*, **128**, 4149–4154, 2000.
- Liebmann, B., and C. A. Smith, Description of a complete (interpolated) outgoing longwave radiation dataset, *Bull. Am. Meteorol. Soc.*, **77**, 1275–1277, 1996.
- Liebmann, B., G. N. Kiladis, J. A. Marengo, T. Ambrizzi, and J. D. Glick, Submonthly convective variability over South America and the South Atlantic Convergence Zone, *J. Clim.*, **12**, 1877–1891, 1999.
- Lobocki, L., A procedure for the derivation of surface-layer bulk relationships from simplified second-order closure models, *J. Appl. Meteorol.*, **32**, 126–138, 1993.
- Manabe, S., Climate and the ocean circulation, I, The atmospheric circulation and the hydrology of the earth's surface, *Mon. Weather Rev.*, **97**, 739–774, 1969.
- Mellor, G. L., and T. Yamada, A hierarchy of turbulence closure models for planetary boundary layers, *J. Atmos. Sci.*, **31**, 1791–1806, 1974.
- Mellor, G. L., and T. Yamada, Development of a turbulence closure model for geophysical fluid problems, *Rev. Geophys.*, **20**, 851–875, 1982.
- Mesinger, F., Forward-backward scheme, and its use in a limited area model, *Contrib. Atmos. Phys.*, **50**, 200–210, 1977.
- Mesinger, F., A blocking technique for representation of mountains in atmospheric models, *Riv. Meteorol. Aeronaut.*, **44**, 195–202, 1984.
- Mesinger, F., and T. Black, On the impact on forecast accuracy of the step-mountain (eta) vs. sigma coordinate, *Meteorol. Atmos. Phys.*, **50**, 47–60, 1992.
- Mesinger, F., Z. I. Janjić, S. Nicković, D. Gavrilov, and D. G. Deaven, The step-mountain coordinate: Model description and performance for cases of Alpine lee cyclogenesis and for a case of an Appalachian redevelopment, *Mon. Weather Rev.*, **116**, 1493–1518, 1988.
- Pan, Z., E. Takle, W. Gutowski, and R. Turner, Long simulation of regional climate as a sequence of short segments, *Mon. Weather Rev.*, **127**, 308–321, 1999.
- Sass, B. H., and J. H. Christensen, A simple framework for testing the quality of atmospheric limited models, *Mon. Weather Rev.*, **123**, 101–113, 1995.
- Sato, N., P. J. Sellers, D. A. Randall, E. K. Schneider, J. Shukla, J. L. Kinter III, Y.-T. Hou, and E. Albertazzi, Effects of implementing the Simple Biosphere Model in a general circulation model, *J. Atmos. Sci.*, **46**, 2757–2782, 1989.
- Satyamurty, P., C. A. Nobre, and P. L. Silva Dias, South America, in *Meteorology of the Southern Hemisphere*, edited by D. J. Karoly and D. G. Vincent, pp. 119–139, Am. Meteorol. Soc., Boston, Mass., 1998.
- Sellers, P. J., Y. Mintz, Y. C. Sud, and A. Dalcher, A simple biosphere model (SiB) for use within general circulation models, *J. Atmos. Sci.*, **43**, 505–531, 1986.
- Seth, A., and F. Giorgi, The effects of domain choice on summer precipitation simulation and sensitivity in a regional climate model, *J. Clim.*, **11**, 2698–2712, 1998.
- Silva, J. T., *Regional estimate of sensible and latent heat fluxes in rainforest and pasture areas in Amazon (in Portuguese)*, M.Sc. thesis, 113 pp., Inst. Nac. de Pesqui. Espaciais, São José dos Campos, Brazil, 1998.
- Slingo, J. M., The development and verification of a cloud prediction scheme for ECMWF model, *Q. J. R. Meteorol. Soc.*, **113**, 899–927, 1987.
- Takle, E. S., et al., Project to intercompare regional climate simulations (PIRCS): Description and initial results, *J. Geophys. Res.*, **104**, 19,443–19,461, 1999.
- Tanajura, C. A. S., *Modeling and analysis of the South American summer climate*, Ph.D. thesis, 164 pp., Univ. of Md., College Park, 1996.
- Tanajura, C. A. S., and J. Shukla, Modeling the effects of the Andes on the South American summer climate, *Tech. Rep. 83*, 44 pp., Cent. for Ocean-Land-Atmos. Stud., College Park, Md., 2000.
- Weisse, R., H. Heyen, and H. von Storch, Sensitivity of a regional atmospheric model to a sea state-dependent roughness and the need for ensemble calculations, *Mon. Weather Rev.*, **128**, 3631–3642, 2000.
- Xie, P. P., and P. A. Arkin, Analyses of global monthly precipitation using gauge observations, satellite estimates, and numerical model predictions, *J. Clim.*, **9**, 840–858, 1996.
- Xue, Y., P. J. Sellers, J. L. Kinter III, and J. Shukla, A simplified biosphere model for global climate studies, *J. Clim.*, **4**, 345–364, 1991.
- Xue, Y., H. G. Bastable, P. A. Dirmeyer, and P. J. Sellers, Sensitivity of simulated surface fluxes to changes in land surface parameterizations: A study using ABRACOS data, *J. Appl. Meteorol.*, **35**, 386–400, 1996.

S. C. Chou and C. A. Nobre, Centro de Previsão de Tempo e Estudos Climáticos (CPTEC), Instituto Nacional de Pesquisas Espaciais (INPE), Cachoeira Paulista, 12630-000 São Paulo, Brazil. (chou@cptec.inpe.br; nobre@cptec.inpe.br)

C. A. S. Tanajura, Laboratório Nacional de Computação Científica (LNCC), Petrópolis, Rio de Janeiro, Brazil. (cast@lncc.br)

Y. Xue, Department of Geography, University of California at Los Angeles (UCLA), Los Angeles, CA, USA. (yxue@geog.ucla.edu)

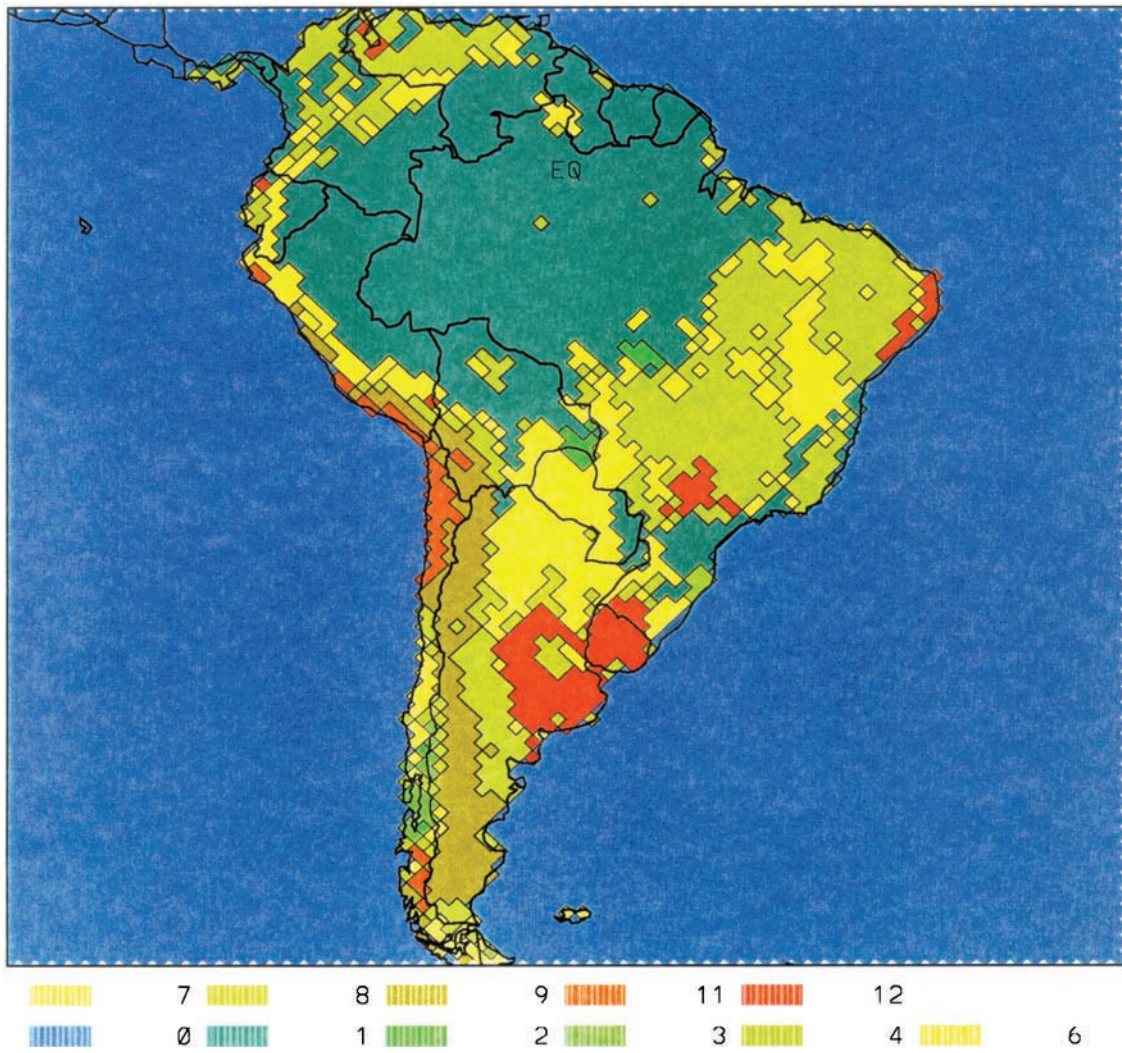


Figure 1. 80-km vegetation map derived from an original 1-km University of Maryland data set.